Angela Bonaccorso

Istituto Nazionale
di Fisica Nucleare
SEZIONE DI PISA

Terzo Incontro Nazionale di Fisica Nucleare
INFN2016

Prospettive della fisica con fasci (dei nuclei) radioattivi

In Italia i gruppi interessati sono:

CSN4 - IS STRENGTH (MI, PD, PI, NA, CT, LNS)

Roca Maza, Mengoni, AB, Coraggio, Verde

medium-heavy nuclei, bulk properties

CSN3- MAGNEX-NUMEN

ASFIN2 (LNS)

EXOTIC (PD, NA),

GAMMA (FI, PD, GE, MI, NA, PG (+CM), LNL)

LNS-STREAM2 (LNS)

NEWCHIM (CT, LNS, ME, MI, NA)

NUCL-EX (FI, BO, LNL, PD, NA)

PRISMA-FIDES (LNL, PD)

~300 stable nuclei, ~ 7000 "exotic"

Half-life data

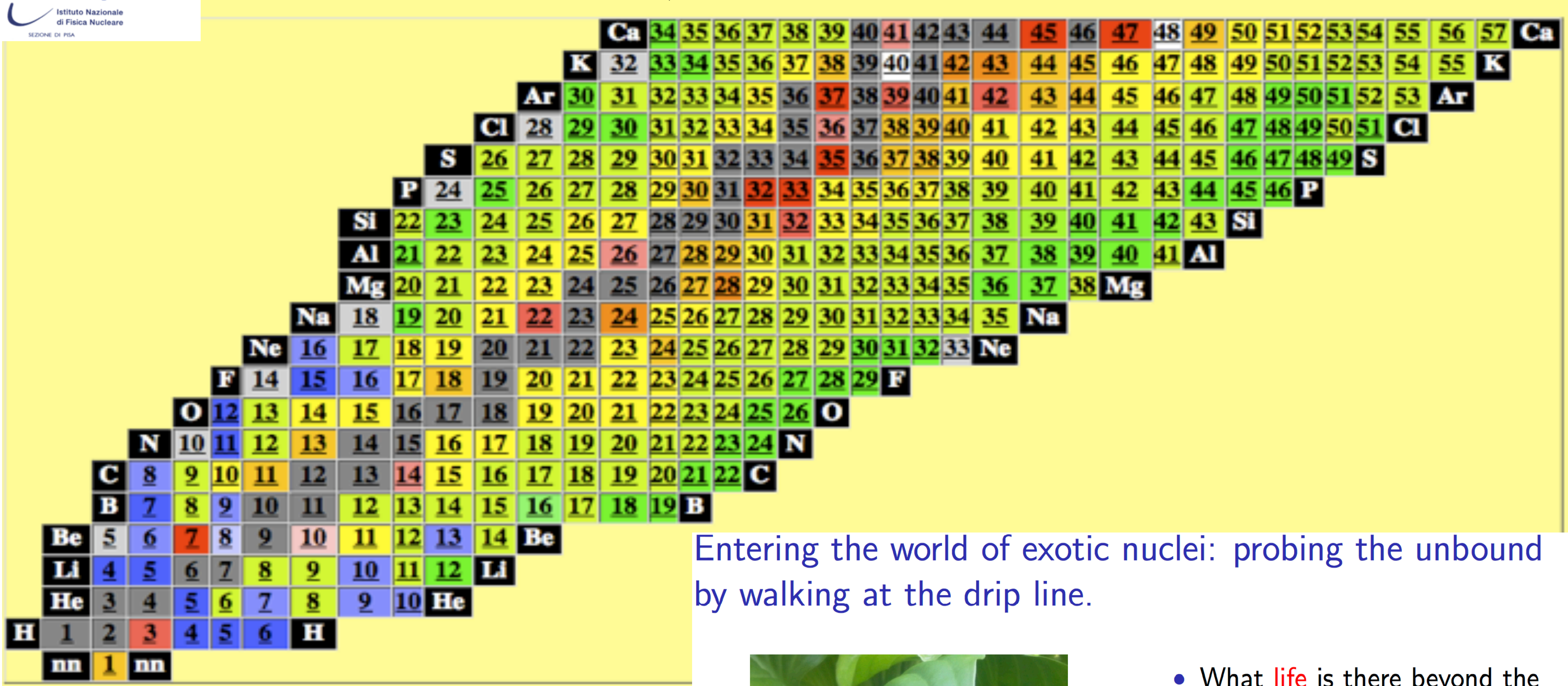

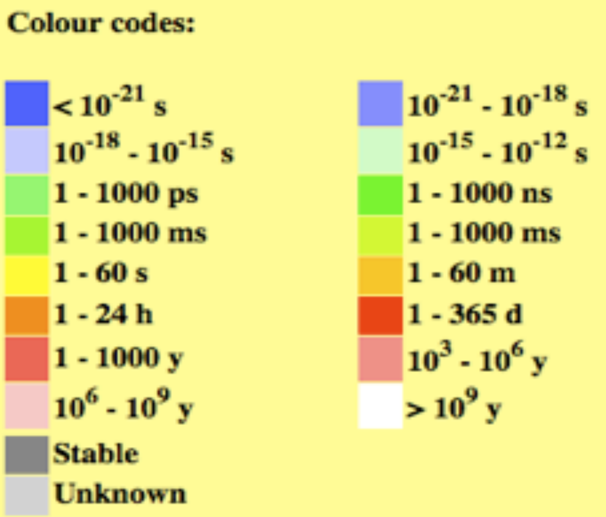

Entering the world of exotic nuclei: probing the unbound by walking at the drip line.

- What life is there beyond the dripline?
- How can we discover it without getting lost?
- Extend our understanding of the *residual* nuclear force.
- Check the limits of validity of structure models such as the SHELL MODEL or "ab initio" models.
- Challenges in peripheral reaction theory.

INFN Angela Bonaccorso
Istituto Nazionale di Fisica Nucleare
SEZIONE DI PISA

Georgio Fea, Il Nuovo Cimento 2, 368 (1935)

TABELLE RIASSUNTIVE E BIBLIOGRAFIA DELLE TRASMUTAZIONI ARTIFICIALI

Nota di GIORGIO FEA (*)

Dato il grande sviluppo preso dallo studio delle trasmutazioni artificiali, sopratutto dopo l'impulso dato dalla scoperta della radioattività provocata, è parso utile, allo scrivente, riassumere in alcune tabelle sinottiche quanto è stato sin qui ottenuto dagli ormai moltissimi ricercatori, che si sono occupati dell'argomento.

Segue un'ampia bibliografia delle opere consultate per la compilazione delle tabelle stesse, e un quadro rappresentante, nel diagramma neutroni-protoni, quanto si conosce circa gli isotopi stabili e radioattivi.

Disposizione delle tabelle.

§ 1. Esse sono quattro, in corrispondenza dei quattro tipi di corpuscoli bombandanti considerati, e cioè:

1) Trasmutazioni ottenute con bombardamento di protoni e deutoni.
2) Trasmutazioni ottenute con bombardamento di nuclei d'elio.
3) Trasmutazioni ottenute con bombardamento di neutroni.
4) Trasmutazioni ottenute con bombardamento di fotoni.

Ciascuna tabella è divisa in otto colonne, nelle quali è riportato, salvo nella seconda parte della terza tabella, quanto segue:

1) l'elemento bombardato, indicato col simbolo chimico e il numero atomico;

2) *a*: la energia del corpuscolo bombardante corrispondente ai dati energetici dei prodotti di trasmutazione riportati nella sesta colonna; questo dato ha importanza particolare per le trasmutazioni con nuclei d'elio, mentre può essere in generale trascurato nel caso di trasmutazioni con protoni e deutoni; perciò esso manca nella prima tabella.

b: in parentesi quadra e con segno > quella che da molti autori è data come energia minima per l'emissione dei corpuscoli indicati accanto in parentesi (se manca l'indicazione del corpuscolo il dato si riferisce alla

(*) Si presentano la bibliografia e le tabelle riassuntive di tutte le trasmutazioni artificiali studiate sino al Maggio 1935.

QUADRO PROTONI-NEUTRONI - I.

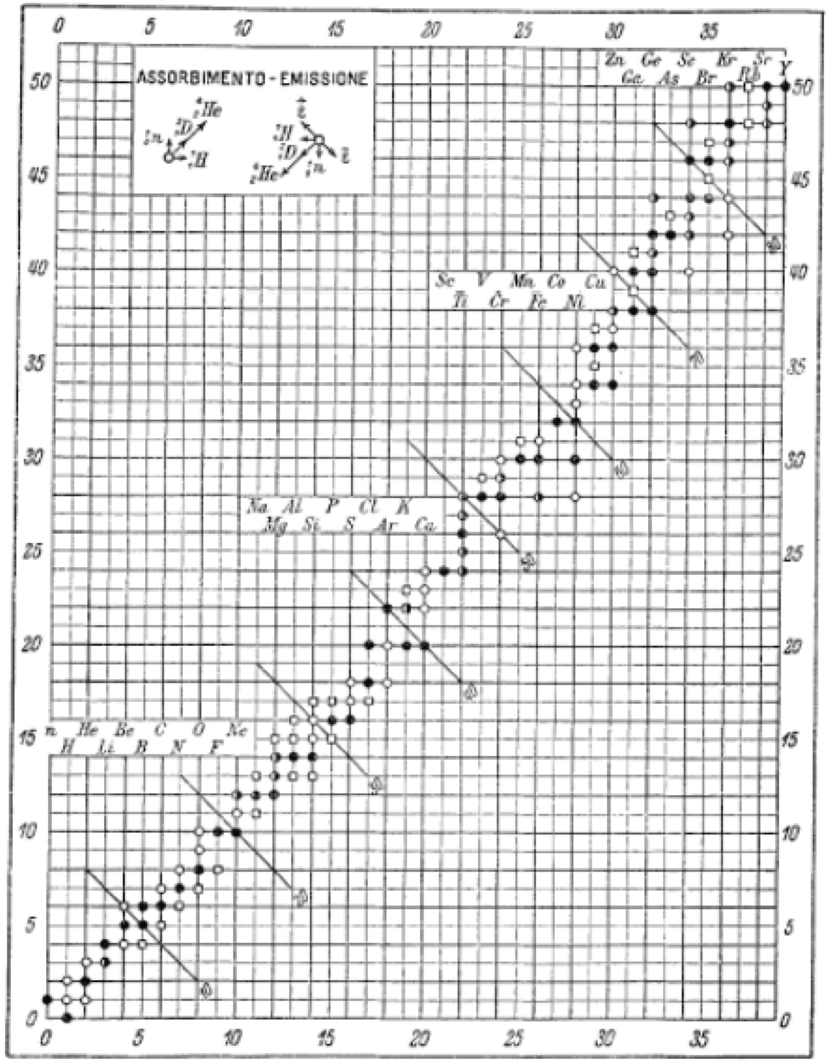

[Carlo Perrier](#) and [Emilio Segrè](#). 43Tecnezio, Palermo 1936

- Fin dall’inizio la fisica nucleare è stata caratterizzata dallo studio della radioattività e quindi dei decadimenti, “complementato`` dallo studio delle proprietà nucleari in funzione della massa (isobari), numero of neutroni (isotope) e/o dei protoni (isotoni). Da qui la necessità di ottenere nuclei con svariate combinazioni del numero di protoni e neutroni.
- I nuclei radioattivi sono del DNA della fisica nucleare, in particolare di quella italiana e sono state solo le difficoltà tecniche nell’ottenerli come fasci che ne ha impedito uno studio più sistematico fin dall’inizio.

RECUPERIAMO IL TEMPO PERDUTO

Rewriting Nuclear Physics textbooks
30 years with Radioactive Ion Beam Physics

Pisa (Italy), July 20th – 24th, 2015

The scope of the activity is twofold. First we will celebrate 30 years since the first genuine work on radioactive ion beams (RIBs) used to study properties of atomic nuclei. Since then Low Energy Nuclear Physics research fed by experiments at various facilities all over the world has experienced a great revival supported by widespread theoretical efforts which have changed deeply our understanding of nuclei and their interactions.
The second scope of the event is to attract and educate the best possible students introducing them to the wonders of Physics with RIBs. We shall try to convey to such students a view of the rich variety of on-going activities in the field, both experimental and theoretical such that the progresses we have made in the last 30 years can be developed further in the future. The planned activities will be directed towards students who are in the process of deciding what graduate studies to specialize.

Program

Isao Tanihata (Osaka and Beijing)	How it all started
Magda Kowalska (CERN, Geneva)	Global properties of atomic nuclei: masses, radii and modern methods to measure them
Riccardo Raabe (Leuven)	Making radioactive ion beams, detecting reaction products
Giovanna Benzoni (Milano)	Strong, weak and electromagnetic forces at work in atomic nuclei, decay properties
Sonia Bacca (TRIUMF, Vancouver)	Structure models: from shell model to ab initio methods
Stefan Typel (GSI)	Reaction theory
Robert J. Charity (St Louis)	Resonance phenomena: from compound nucleus decay to proton radioactivity
Tomohiro Uesaka (RIKEN)	Experimental methods and measured observables with polarized proton targets: understanding spin-orbit
Alexandre Obertelli (Saclay)	Probing nuclear structure with direct reactions: observables, methods and recent progress with rare isotopes
Andrea Jungclaus (Madrid)	Single particle versus collectivity, shapes of exotic nuclei
Lucio Gialanella (Napoli)	Radioactive ion beams in experimental nuclear astrophysics
Ulli Koester (ILL-Grenoble)	Applications of physics of unstable nuclei to energy, medicine, material science
Bjorn Jonson (Göteborg)	What's next in Nuclear Physics with RIBs

24/7/2015: Visit to the INFN Legnaro National Laboratory where SPES, the Italian RIB's facility is under construction

Local Organizing Committee

Angela Bonaccorso, INFN, Pisa (co-chair)
Giovanni Casini, INFN, Firenze (co-chair)
Ignazio Bombaci, Department of Physics, University of Pisa
Alejandro Kievsky, INFN, Pisa
Laura Elisa Marcucci, Department of Physics, University of Pisa
Valeria Rosso, Department of Physics, University of Pisa
Michele Viviani, INFN, Pisa

Lucia Lilli and Claudia Tofani, INFN, Pisa (Secretaries): ExoticNuclei2015@pi.infn.it

http://exotic2015.df.unipi.it

Università di Pisa

INFN Istituto Nazionale di Fisica Nucleare

Poster designer: Ignazio Bombaci

EPJ Plus

Focus Point on Rewriting Nuclear Physics textbooks: 30 years with radioactive ion beam physics

N. Alamanos, C. Bertulani, A. Bracco, A. Bonaccorso, D. Brink and G. Casini

Nuclear Physics with RIB's: How it all started
Isao Tanihata
Eur. Phys. J. Plus, 131 4 (2016) 90

Making radioactive ion beams - Detecting reaction products
Riccardo Raabe
Eur. Phys. J. Plus, 131 10 (2016) 362

Global properties of atomic nuclei - Masses, radii and modern methods to measu
Magdalena Kowalska
Eur. Phys. J. Plus, 131 8 (2016) 294

Strong, weak and electromagnetic forces at work in atomic nuclei, decay propert
G. Benzoni
Eur. Phys. J. Plus, 131 4 (2016) 99

Structure models: From shell model to ab initio methods - A brief introduction to microscopic theories for exotic nuclei
Sonia Bacca
Eur. Phys. J. Plus, 131 4 (2016) 107

Single particle versus collectivity, shapes of exotic nuclei
Andrea Jungclaus
Eur. Phys. J. Plus, 131 3 (2016) 59

Reaction theory
Stefan Typel
Eur. Phys. J. Plus, 131 1 (2016) 13

Resonance phenomena: From compound nucleus decay to proton radioactivity
R. J. Charity
Eur. Phys. J. Plus, 131 3 (2016) 63

Spins in Exotic Nuclei: RI-beam Experiments with Polarized Targets
T. Uesaka
Eur. Phys. J. Plus, (2016) in press.

Nuclear structure from direct reactions with rare isotopes: observables, methods and highlights
Alexandre Obertelli
Eur. Phys. J. Plus, 131 9 (2016) 319

Radioactive ion beams in nuclear astrophysics
L. Gialanella
Eur. Phys. J. Plus, 131 9 (2016) 331

What's next in nuclear physics with RIB's
Björn Jonson
Eur. Phys. J. Plus, 131 2 (2016) 20

Queste sono le nostre prospettive e speranze per il futuro

"SPES is a project where I can foresee that many of the participating students in our school will have their future research activities, in particular those coming from Italy. It is a gift to have a National Laboratory of this class and we are all looking forward to see how it will develop.``. **From B. Jonson's talk**

Partners

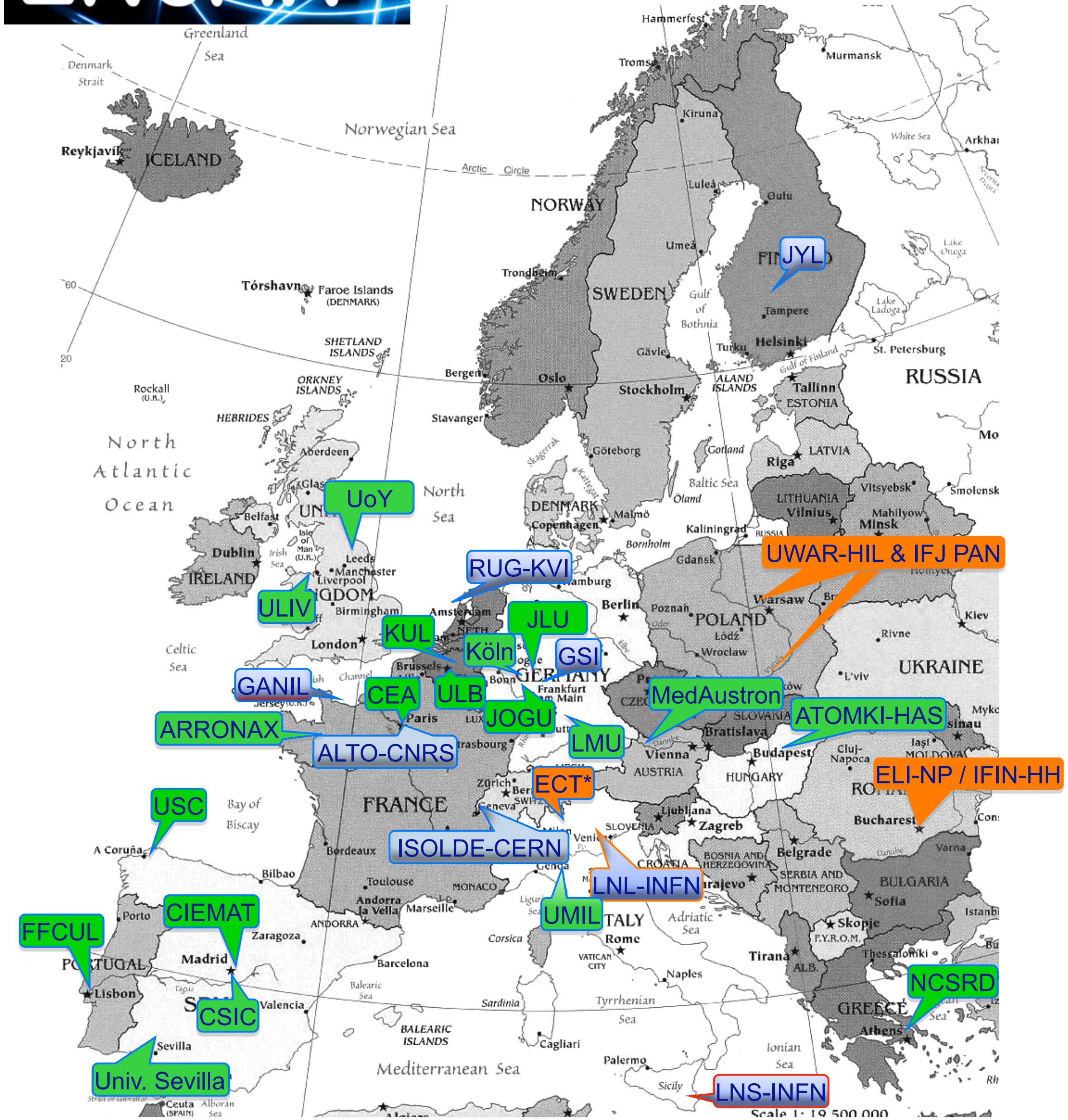

10 TNA Facilities

30 beneficiaries
15 countries

Community: 2700-3000 scientists and highly qualified engineers

Close collaboration with infrastructures outside Europe:
Canada: TRIUMF Vancouver
China: IMP Lanzhou
India: BARC Mumbai
VECC Calcutta
Japan: RIKEN Tokyo
RCNP Osaka
Russia: JINR Dubna
South Africa: iThemba Cape Town
United States: NSCL East Lansing
ANL Argonne

INFN Angela Bonaccorso
Istituto Nazionale di Fisica Nucleare
SEZIONE DI PISA

Total budget of ENSAR2 is 10ME (3.25ME pre-financing)

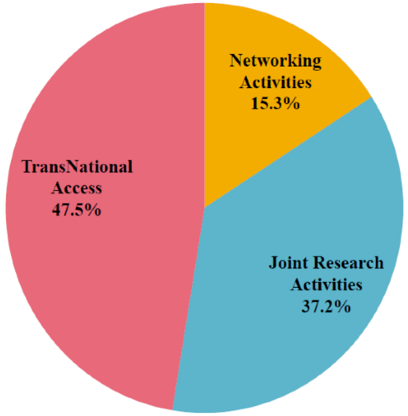

8 Networks

- NA1 - FISCO2: FInancial and SCientific Organisation
- NA2 - NUSPRASEN: Nuclear Structure Physics, Reactions, Astrophysics and Superheavy Elements Network
- NA3 – MIDAS: MInimisation of Destructive plASma processes in ECRIS
- NA4 – NUSPIN: Nuclear SPectroscopy INstrumentation
- NA5 – MediNet: Medical Network
- NA6 – GDS: Gas-Filled Detectors and Systems
- NA7- ENSAF: European Network of Small-scale Accelerator Facilities
- NA8 – NuPIA: Nuclear Physics InnovAtion

7 JRAs

- JRA1 – PASPAG: Phoswich scintillator assemblies: Application to the Simultaneous detection of PArticle and Gamma radiation
- JRA2 - PSeGe: R&D on Position-Sensitive Germanium Detectors for Nuclear Structure and Applications
- JRA3 - TheoS: Theoretical Support for Nuclear Facilities in Europe
- JRA4 - RESIST : RESonance laser Ionisation Techniques for separators
- JRA5 - SATNuRSE: Simulations and Analysis Tools for Nuclear Reactions and Structure in Europe
- **JRA6 - EURISOL**
- JRA7 – TecHIBA: Technologies for High Intensity Beams and Applications

Angela Bonaccorso

JRA EURISOL, WP14

WP leader: Yorick Blumenfeld (IN2P3-IPNO)

Deputy WP leader: Fredrik Wenander (CERN)

Participants and Management

Participants: CERN, GANIL, HIL Warsaw, IFJ Krakow, IN2P3 – IPNO, INFN – LNL.

Steering committee: WP leader + 1 representative per participant

Alberto Andrighetto (INFN – LNL Legnaro)

Piotr Bednarczyk (IFJ,Krakow)

Yorick Blumenfeld (IN2P3-IPNO, WP leader)

Manssour Fadil (GANIL)

Przemysław Gmaj (HIL Warsaw)

Maher Cheikh Mhamed (IN2P3-IPNO)

Fredrik Wenander (CERN, deputy WP leader)

Total EC budget: 640 K€

Objectives and Structure

EURISOL concept defined during EURISOL DS (2005-2009) : NuPECC LRP priority

JRA includes R&D

Necessary for future EURISOL

which will enhance output of ENSAR2 ISOL facilities, in particular SPIRAL & SPIRAL2, HIE-ISOLDE, SPES and ALTO see also **EURISOL DF**

Includes 3 tasks:

. ICBT: Innovative Charge Breeding Techniques

. Beamlab: Development of chemically reactive nuclear beams

. CRIBE: Chart of Radioactive Ion Beams in Europe

EURISOL User Group

Will keep updated the physics case with meet in particular a town meeting in PISA, spring 2

User Executive Committee

- **Berta Rubio, Spain; chair**

Didier Beaumel, France;
Maria Borge, CERN;
Giacomo de Angelis, Italy;
Lidia Ferreira, Portugal;
Adam Maj, Poland;
Iain Moore, Finland;
Riccardo Raabe, Belgium;
Haik Simon, Germany.

AB, NUSPRASEN ex-officio representative.

In particolare ci interessa CRIBE (Chart of Radioactive Ion Beams in Europe)

Task leader : M. Fadil (GANIL)

Participants: GANIL, IFJ Krakow

Which criteria for RIBs to consider in CRIBE ?

The main idea of this activity is to collect available data (essentially intensities and energies) of radioactive-ion beams produced in the existing European ISOL facilities dedicated to the production and the acceleration of RIBs. Both low-energy (at the exit of a mass separator) and post-accelerated RIBs will be taken into account. These data will be accessible and visualized through a nuclear chart. The experience already gained at GANIL in this type of project will be used to carry out this project successfully. This chart will present beams that are already available in the nuclear facilities (ALTO, GANIL, GSI (low energy), ISOLDE, Jyväskylä, LNL, ELI-NP?) or that will become available during the ENSAR2 mandate.

Courtesy of T. Motobayashi

Asian activity expanding

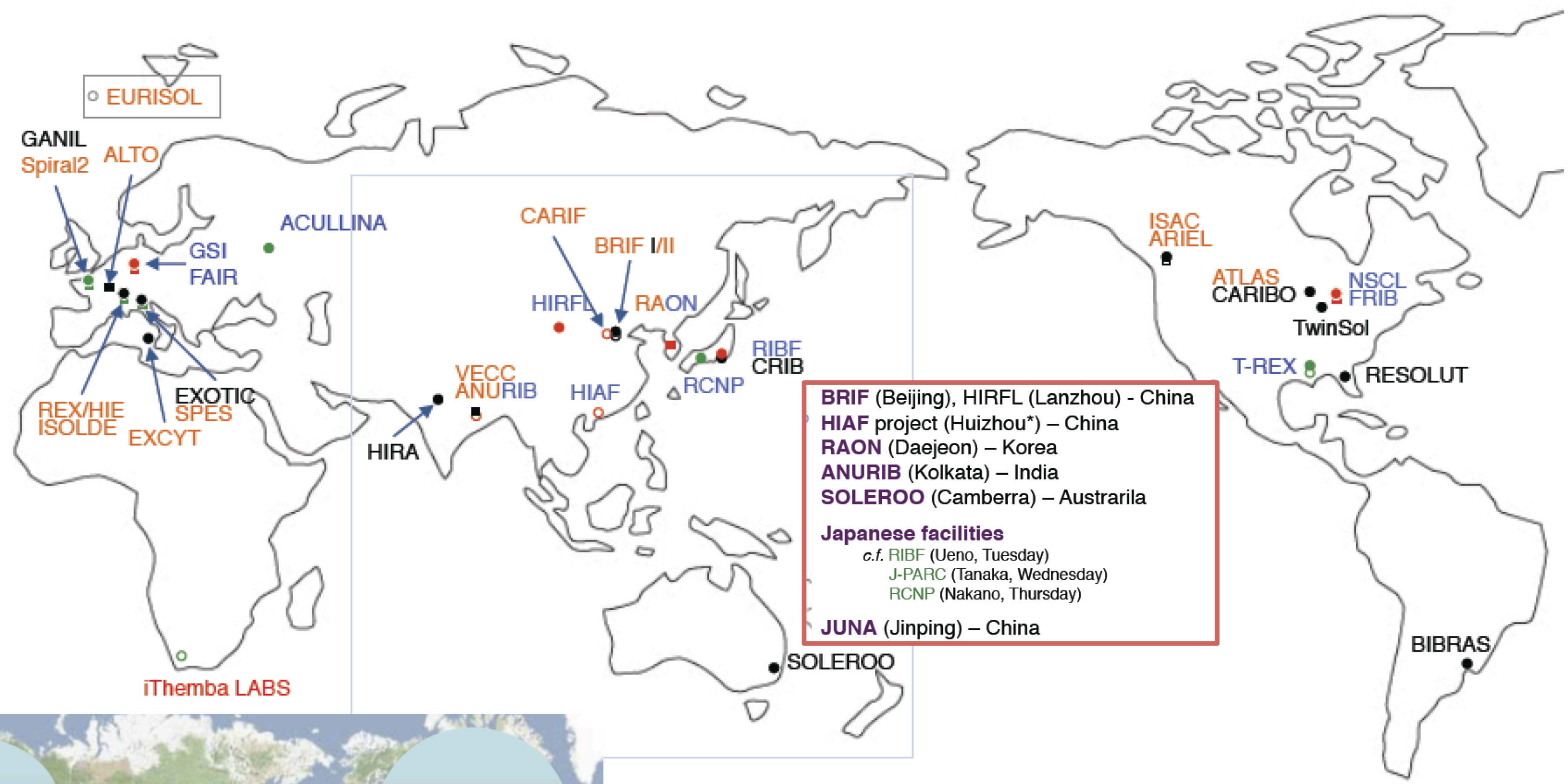

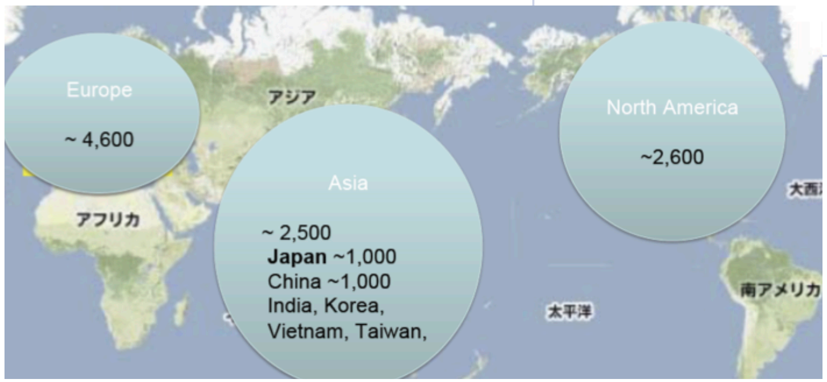

World map of RI beam facilities

Experimental data vs. **Reaction theory** vs. Structure theory

- Direct reactions involve few nucleons and few degrees of freedom but to "model" them requires understanding the whole nucleus and all other possible reactions. Ex: **elastic scattering and the optical potential.**
- It requires also the understanding of **experimental setups** and the handling of data to extract meaningful observables.
- It has to be **simple and transparent** in its interpretation to help disentangling the physical processes and allow experimentalists to describe their data.
- Reaction theorists must understand **stucture models,** experiments and they must describe data reliably but in a simple way.

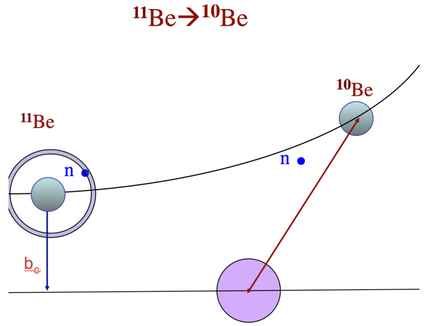

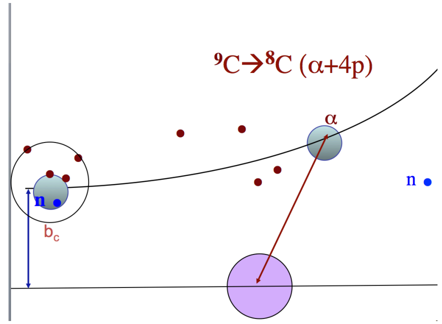

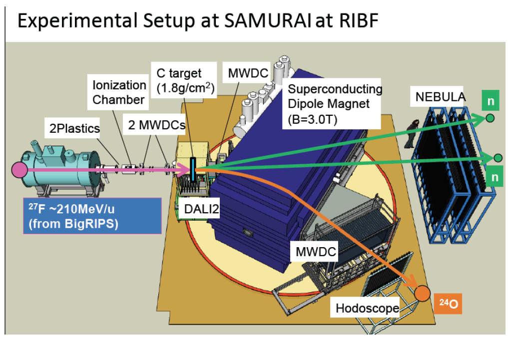

HiRA array

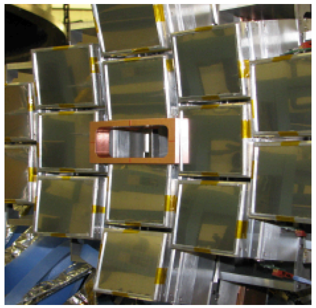

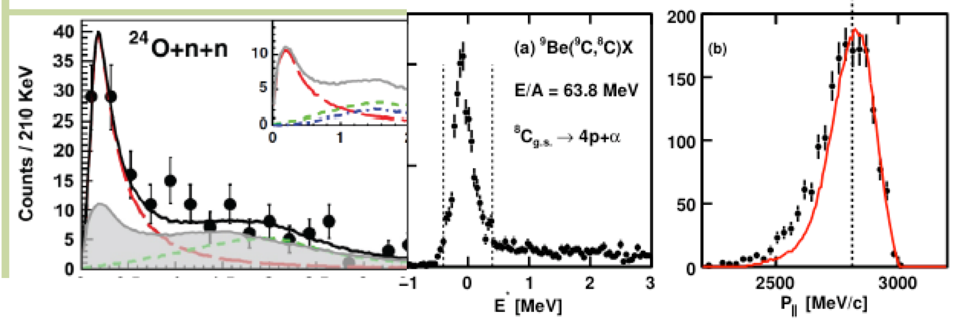

Direct ractions and projectile breakup in particular are important in astrophysics and for practical applications. The International Atomic Energy Agency recently completed a Coordinated Research Project (CRP) to update the Fusion Energy Nuclear Data Library

INFN Angela Bonaccorso
Istituto Nazionale di Fisica Nucleare
SEZIONE DI PISA

$^{11}Be \rightarrow {}^{10}Be$

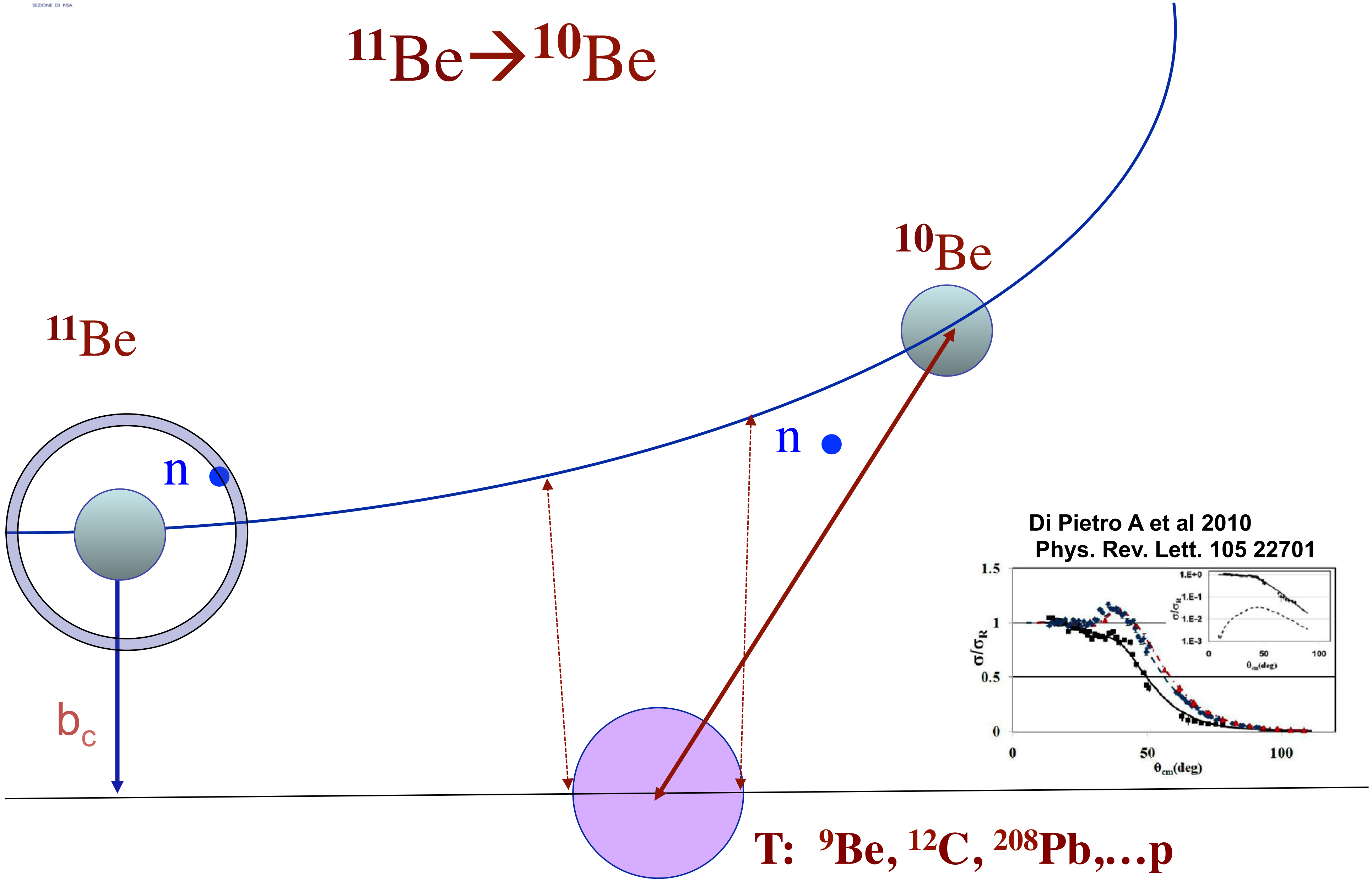

INFN Angela Bonaccorso
Istituto Nazionale di Fisica Nucleare
SEZIONE DI PISA

$^{9}C \rightarrow {}^{8}C\ (\alpha+4p)+n$

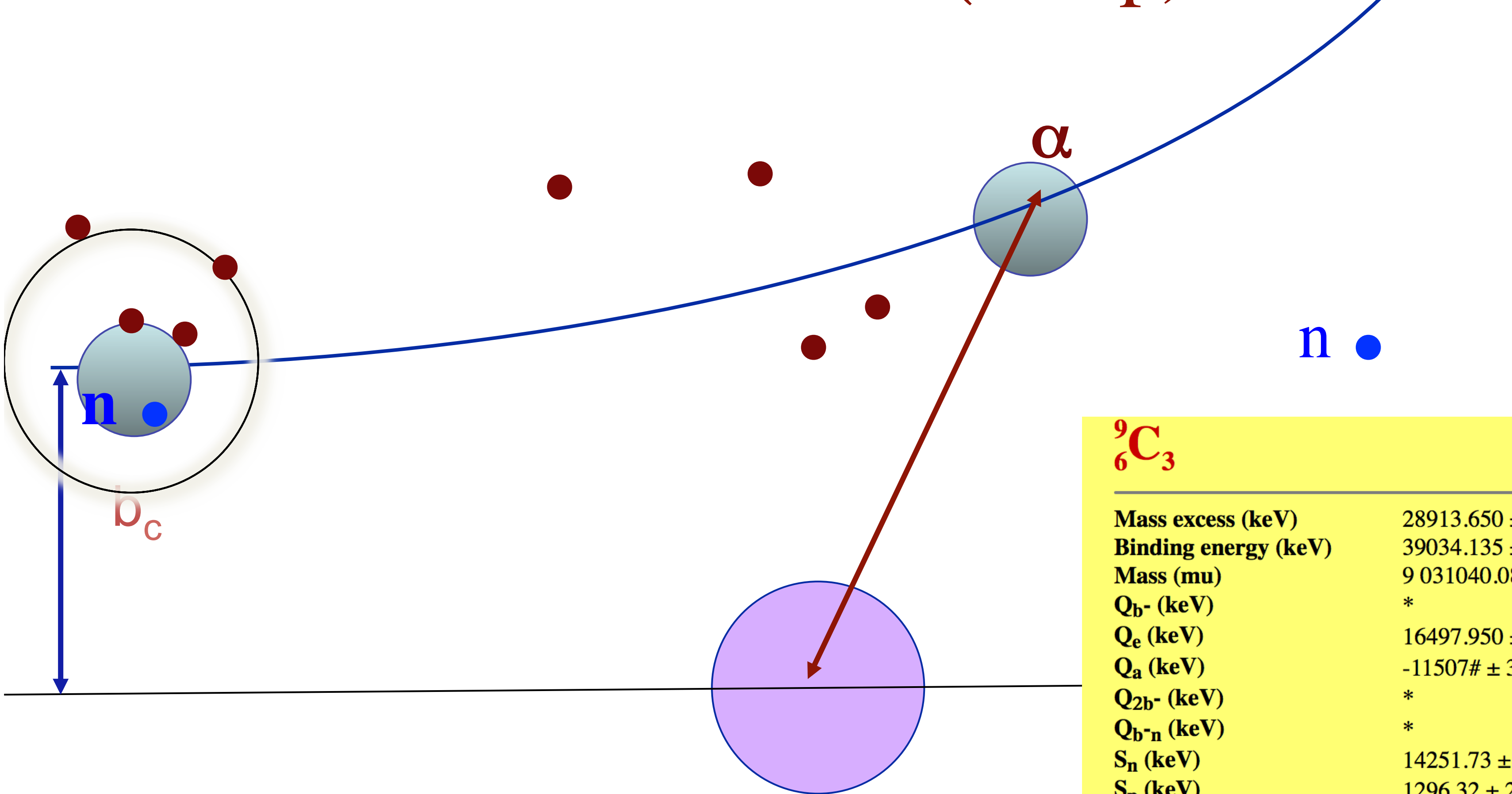

$^{9}_{6}C_{3}$

Mass excess (keV)	28913.650 ± 2.178
Binding energy (keV)	39034.135 ± 2.178
Mass (mu)	9 031040.087 ± 2.338
Q_b- (keV)	*
Q_e (keV)	16497.950 ± 2.374
Q_a (keV)	-11507# ± 3996#
Q_{2b}- (keV)	*
Q_{b^-n} (keV)	*
S_n (keV)	14251.73 ± 23.17
S_p (keV)	1296.32 ± 2.35
S_{2n} (keV)	*
S_{2p} (keV)	1433.78 ± 2.13

Proton unbound nuclei via invariant mass method

Interest: Two-proton radioactivity vs. 2n-halo by isospin symmetry
^{5}He, ^{6}He,^{8}He,^{12}Be and IMME

Isobaric Multiplet Mass Equation

Proton unbound nuclei

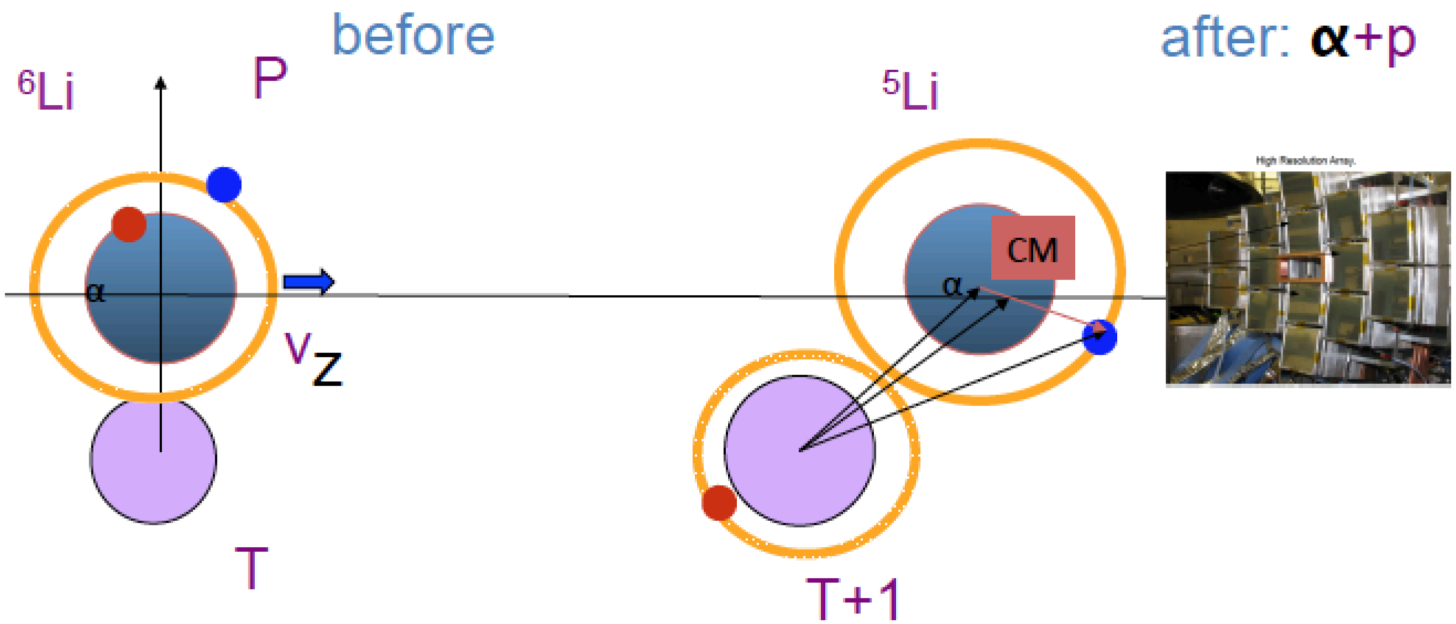

^{6}Li,^{7}Be,^{9}C,^{13}O studied by knockout of a deeply bound **neutron**:

R. J. Charity & HiRA collaboration

Another motivation

p-p chain

$$p(p,\ \beta^+\nu)d(p,\gamma)^3He(\alpha,\gamma)^7Be(p,\gamma)^8B(p,\gamma)^9C(\beta^+\nu)^9B(p)^8Be(\alpha)\alpha.$$

Determine ANC and/or spectroscopic factor for s.p. states
(can give reaction rates directly)
Ab-initio (i.e. Nollett-Wiringa) or HF wfs

NP1412-SAMURAI29R1 (re-evaluation: NP0906-RIBF13)

Title: Inclusive and exclusive breakup of ^{9}C in nuclear and Coulomb fields

Spokesperson: Livius Trache

Approved —Grade A 3 days (including 0.5 days for the BigRIPS tuning)

Collaborators:
F. Carstoiu, RJ Charity
C. Bertulani, T. Motobayashi, L. Sobotka, L. Trache
[Bucharest, St Louis, RIKEN, Texas-Commerce, Pisa]

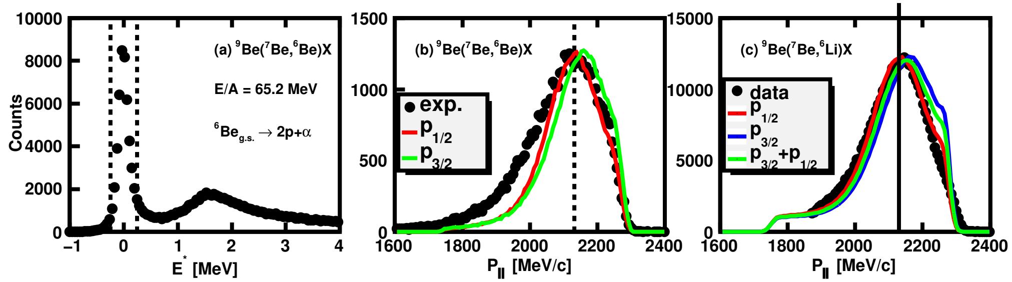

FIGURE 2. (a) Experimental ^{6}Be invariant-mass spectrum and (b,c) the parallel-momentum distributions [3] of the reactions ^{9}Be(^{7}Be,^{6}Be)X, ^{9}Be(^{7}Be,^{6}Li)X at mid-target energy of 65.2*A*MeV. Here and the following figures the dashed line on the $P_{||}$ spectra indicates the momentum of the unreacted beam. The dashed lines in (a) show the gate on the ^{6}Be ground state.

	E_{inc} AMeV	σ_{exp} mb
$\langle ^7Be \mid ^6Be_{g.s} \rangle$	65.2	10
$\langle ^7Be \mid ^6Li_{g.s} \rangle$	65.2	50
$\langle ^9C \mid ^8C_{g.s} \rangle$	63.8	3.82
$\langle ^9C \mid ^8B_{g.s} \rangle$	64.4	54.5
$\langle ^9C \mid ^8B_{1^+} \rangle$	64.4	12.2
$\langle ^9C \mid ^8B_{3^+} \rangle$	64.4	42.6

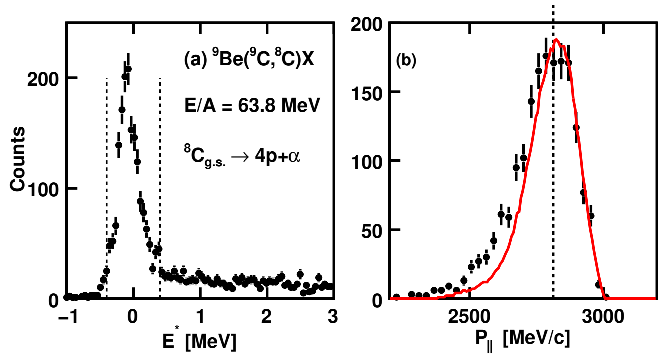

FIGURE 3. (a) The experimental ^{8}C invariant-mass spectrum and (b) the parallel-momentum distributions [3] of the reactions ^{9}Be(^{9}C,^{8}C)X at mid-target energy of 63.8*A*MeV. The gate on the ground state of ^{8}C is indicated by the dashed lines in (a)

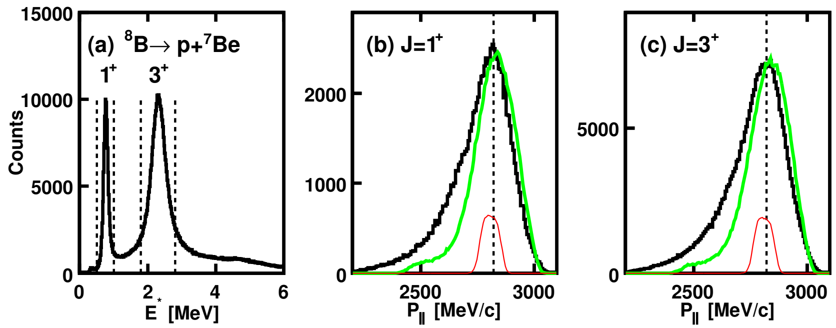

FIGURE 4. (a) The experimental ^{8}B invariant-mass spectrum for the p+^{7}Be channels and (b,c) the parallel-momentum distributions [3] of the reaction ^{9}Be(^{9}C,^{8}B$_{1^+}$)X and ^{9}Be(^{9}C,^{8}B$_{3^+}$)X at 64.4*A*MeV.

Perfect example of most discussed reaction mechanisms vs. structure topics of present day physics with RIBs

- Unbound nuclei
- n-knockout from deeply bound states
- Reduced cross sections
- Elastic scattering
- Total reaction cross sections

transfer and inelastic excitations

A consistent formalism for all breakup reaction mechanisms

The core-target movement is treated in a semiclassical way, but neutron-target and/or neutron-core with a full QM method.

AB and DM Brink, PRC38, 1776 (1988), PRC43, 299 (1991), PRC44, 1559 (1991).

Early eikonal model: I. Tanihata, Prog. Part. Nucl. Phys. 35, 505 (1995), halo-core decoupling.

$$\frac{d\sigma}{d\xi} = C^2 S \int_0^\infty d\mathbf{b_c} \frac{dP_{-n}(b_c)}{d\xi} P_{ct}(b_c),$$

$\otimes$

$$\xi \to \varepsilon_f, k_z, P_{//} \quad also \quad ANC = \sqrt{C^2 S C_i^2}$$

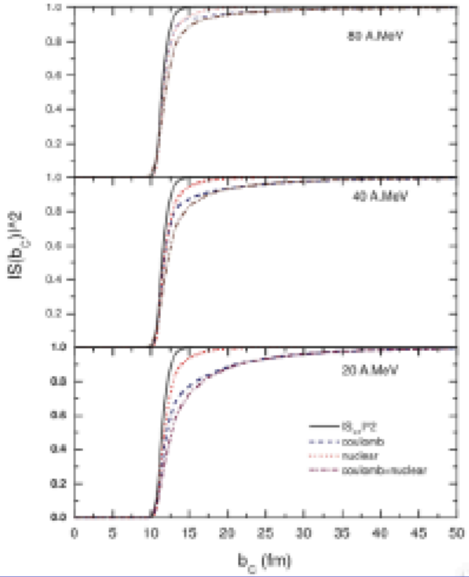

Use of the simple parametrization

$$P_{ct}(b_c) = |S_{ct}|^2 = e^{(-\ln 2 exp[(R_s - b_c)/a])},$$

$$R_s \approx r_s(A_p^{1/3} + A_t^{1/3}) \qquad r_s \approx 1.4 fm$$

'strong absorption radius'

AB&F.Carstoiu, NPA706 (2002) 322
AB&A.Ibraheem, NPA748 (2005) 414

Transfer to the continuum: from resonances to knockout reactions

First order time dependent perturbation theory amplitude: **

$$A_{fi} = \frac{1}{i\hbar} \int_{-\infty}^{\infty} dt < \phi_f(\mathbf{r})|V(\mathbf{r})|\phi_i(\mathbf{r} - \mathbf{R}(t)) > e^{-i(\omega t - mvz/\hbar)} \qquad (1)$$

$$\omega = \varepsilon_i - \varepsilon_f + \tfrac{1}{2}mv^2 \qquad \mathbf{R}(t) = \mathbf{b_c} + vt$$

$$\begin{aligned} \frac{dP_{-n}(b_c)}{d\varepsilon_f} &= \frac{1}{8\pi^3}\frac{m}{\hbar^2 k_f}\frac{1}{2l_i+1}\Sigma_{m_i}|A_{fi}|^2 \\ &\approx \frac{4\pi}{2k_f^2}\Sigma_{j_f}(2j_f+1)(|1-\bar{S}_{j_f}|^2 + 1 - |\bar{S}_{j_f}|^2)\mathcal{F}, \end{aligned}$$

ϕ_f see (*)

$$\mathcal{F} = (1 + F_{l_f,l_i,j_f,j_i})B_{l_f,l_i} \qquad B_{l_f,l_i} = \frac{1}{4\pi}\left[\frac{k_f}{mv^2}\right]|C_i|^2 \frac{e^{-2\eta b_c}}{2\eta b_c} M_{l_f l_i}$$

INFN Angela Bonaccorso
Istituto Nazionale di Fisica Nucleare
SEZIONE DI PISA

Status of the Art

Reaction cross sections of unstable nuclei

Constrain the (nucleus-nucleus) S-matrix $|S|^2$ by total reaction cross section calculations vs exp. data

See for example

http://www.sinap.ac.cn/china-japan/

A. Ozawa (University of Tsukuba)

Also

C. Xiangzhou, F. Jun, S.Wenqing, M. Yugang,W. Jiansong, and Y. Wei, Phys. Rev. C58 (1998) 572.

G. W. Fan et al., Phys. Rev. C90 (2014) 044321.

M. Fukuda et al., Nucl. Phys. A656 (1999) 209.

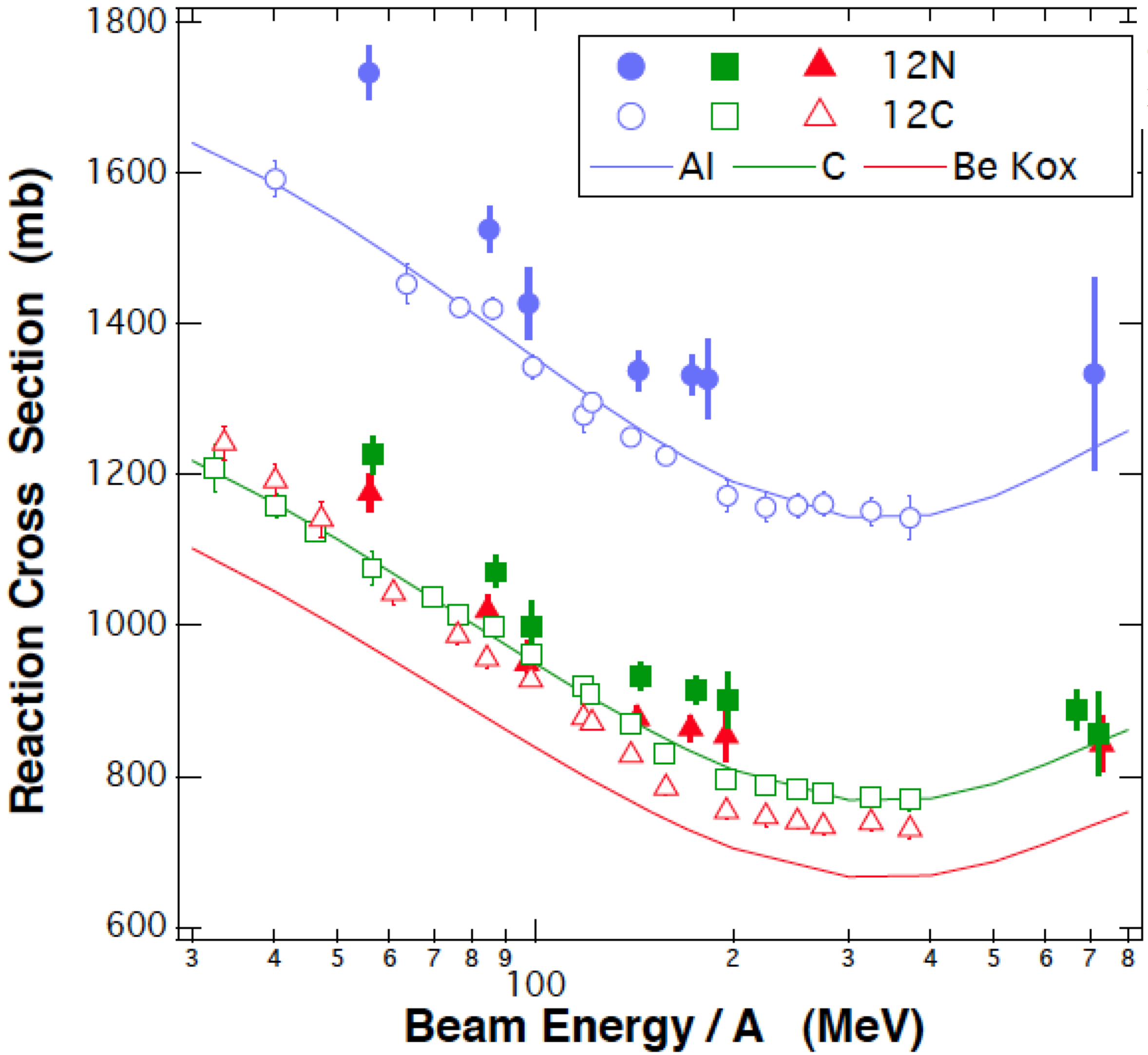

Nuclide	Z	N	S_n (keV)	S_p (keV)
^{12}C	6	6	18721.85 ± 0.95	15956.95 ± 0.42

Nuclide	Z	N	S_n (keV)	S_p (keV)
^{12}N	7	5	15693.76 ± 180.00	601.42 ± 1.38

Proc. Conf. Advances in Radioactive Isotope Science (ARIS2014)
JPS Conf. Proc. **6**, 030103 (2015)
http://dx.doi.org/10.7566/JPSCP.6.030103

Nucleon Density Distribution of the Proton Drip-Line Nucleus ^{12}N Studied via Reaction Cross Sections

Mitsunori Fukuda[1], Yusuke Morita[1], Daiki Nishimura[2], Maya Takechi[3], Kodai Iwamoto[1], Masaru Wakabayashi[1], Yasuto Kamisho[1], Junichi Ohno[1], Masaomi Tanaka[1], Ryosuke Kanbe[1], Shintaro Yamaoka[1], Mototsugu Mihara[1], Kensaku Matsuta[1], Kenta Yoshinaga[2], Ifan Zhu[2], Junpei Khono[4], Sayaka Yamaki[4], Takeshi Suzuki[4], Takayuki Yamaguchi[4], Shinji Suzuki[6], Masayuki Nagashima[3], Kohsuke Abe[3], Keisuke Tashiro[3], Akira Honma[3], Takashi Ohtsubo[3], Takuji Izumikawa[5], Shinji Sato[6], Shigekazu Fukuda[6], and Atsushi Kitagawa[6]

A target used very often is ^{9}Be → single folding of a n-^{9}Be phenomenological potential with a microscopic projectile density

PHYSICAL REVIEW C **94**, 034604 (2016)

Imaginary part of the ^{9}C-^{9}Be single-folded optical potential

A. Bonaccorso,[1,*] F. Carstoiu,[2] and R. J. Charity[3]

Few-Body Syst (2016) 57:331–336
DOI 10.1007/s00601-016-1082-4

**A. Bonaccorso · F. Carstoiu · R. J. Charity · R. Kumar
G. Salvioni**

Differences Between a Single- and a Double-Folding Nucleus-^{9}Be Optical Potential

The Glauber reaction cross section is given by

$$\sigma_R = 2\pi \int_0^\infty b\, db(1 - |S_{NN}(\mathbf{b})|^2) \quad (1)$$

where

$$|S_{NN}(\mathbf{b})|^2 = e^{2\chi_I(b)} \quad (2)$$

is the probability that the nucleus-nucleus (NN) scattering is elastic for a given impact parameter $\mathbf{b}$.

The imaginary part of the eikonal phase shift is given by

$$\chi_I(\mathbf{b}) = \frac{1}{\hbar v}\int dz\, W^{NN}(\mathbf{b}, z) = \frac{1}{\hbar v}\int dz \int d\mathbf{r_1} W^{nN}(\mathbf{r_1} - \mathbf{r})\rho(\mathbf{r_1}) \quad (3)$$

where W^{NN} is negative defined as

$$W^{NN}(\mathbf{r}) = \int d\mathbf{b_1} W^{nN}(\mathbf{b_1} - \mathbf{b}, z) \int dz_1\, \rho(\mathbf{b_1}, z_1). \quad (4)$$

In the double-folding method, W^{NN} is obtained from the microscopic densities $\rho_{p,t}(\mathbf{r})$ for the projectile and target respectively and an energy-dependent nucleon-nucleon (nn) cross section σ_{nn}, i.e.,

$$W^{NN}(\mathbf{r}) = -\frac{1}{2}\hbar v \sigma_{nn} \int d\mathbf{b_1}\, \rho_p(\mathbf{b_1} - \mathbf{b}, z) \int dz_1\, \rho_t(\mathbf{b_1}, z_1). \quad (5)$$

Also

$$W^{nN}(\mathbf{r}) = -\frac{1}{2}\hbar v \sigma_{nn} \rho_t(\mathbf{r}) \quad (6)$$

is a single-folded zero-range n-target imaginary potential and v is the nucleon-target velocity of relative motion. The W^{nN} potential of Eq.(6) has the same range as the target density because σ_{nn} is a simple scaling factor.

Advantages with respect to double folding models:

- The imaginary potential is correctly second order because of the phenomenological nature of the n-T potential.
- The projectile density can be better tested because one is free from the ambiguity on the target density.
- The ambiguity on the nucleon-nucleon interaction to be used is overcome.
- The energy dependence of the potential is correctly reproduced because of the underlying correctness of the n-T potential.
- Deformation and surface effects of the target are correctly taken into account and one is left with the task of modelling the same effects for the exotic projectile.

A.B & R. J. Charity, PRC89, 024619 (2014)

Resonances described by $$\delta V(r) = 16\alpha \frac{e^{2(r-R^R)/a^R}}{(1+e^{(r-R^R)/a^R})^4}.$$ consistent with dispersive contribution

n-^{9}Be scattering data + calculations

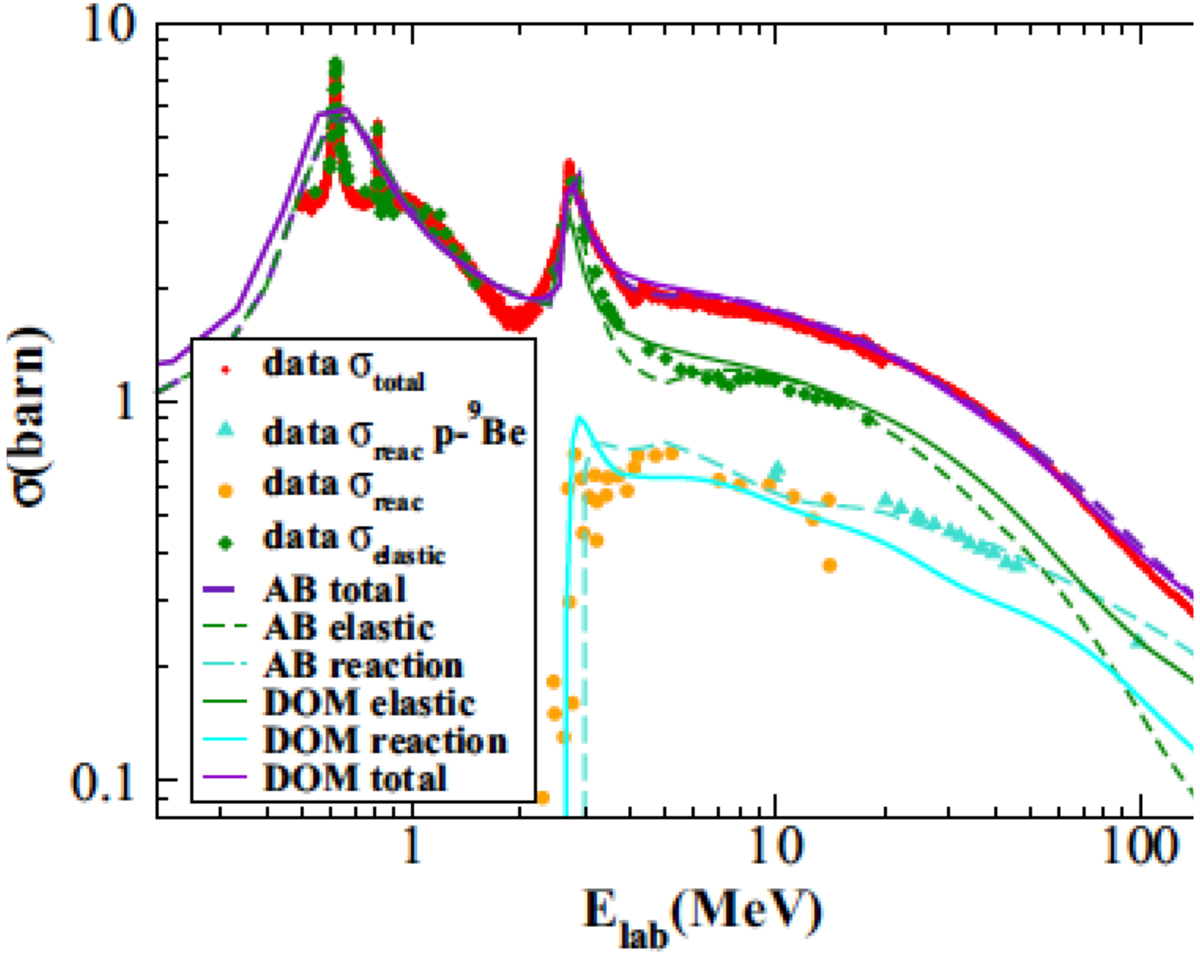

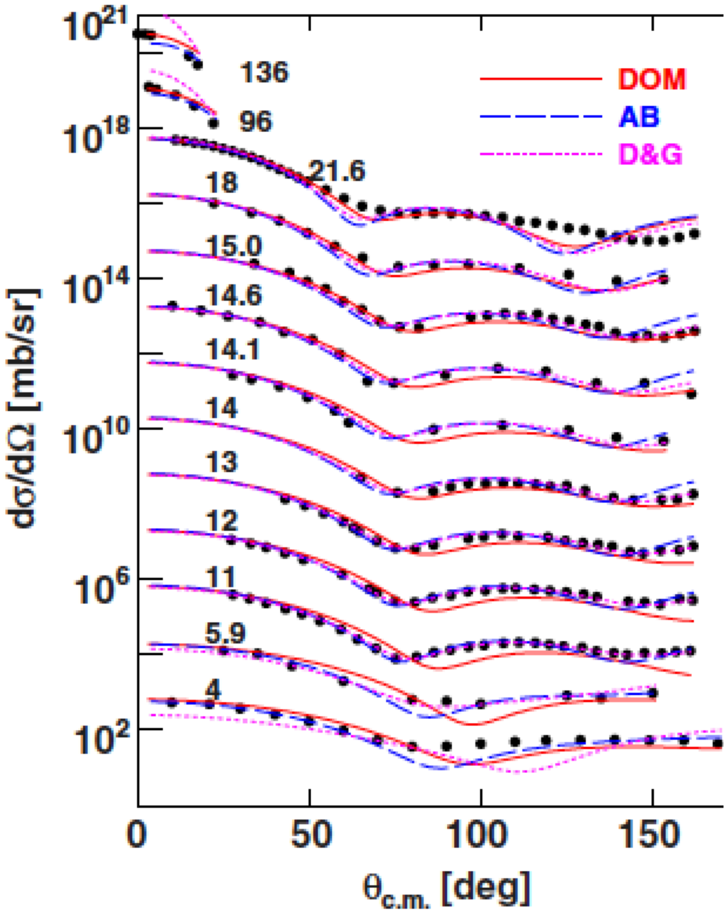

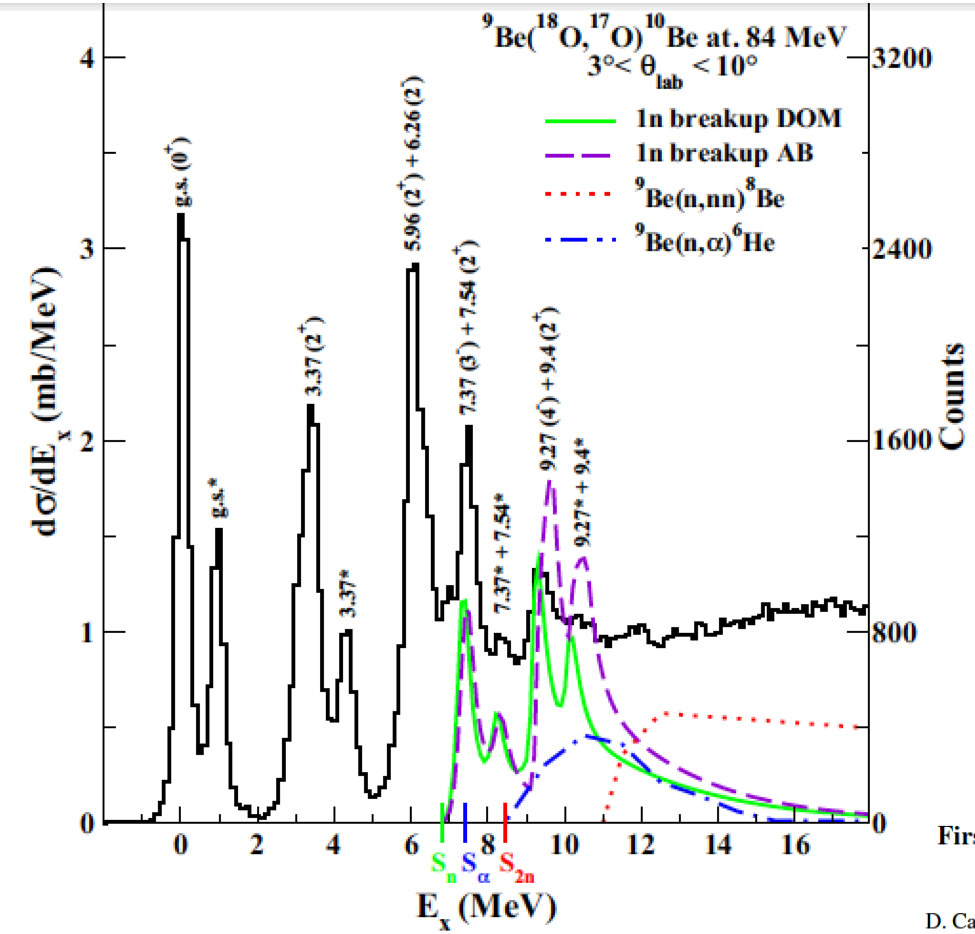

FIG. 2. (Color online) Inclusive excitation energy spectrum of the ^{9}Be(^{18}O, ^{17}O)^{10}Be reaction at 84-MeV incident energy and $3^\circ < \theta_{\rm lab} < 10^\circ$. The background that comes from ^{12}C and ^{16}O impurities has been subtracted. Peaks marked with an asterisk refer to the ^{17}O ejectile emitted in its first excited state at 0.87 MeV. Total $1-n$ breakup calculations that result from the use of the DOM and the AB potentials (see text) [12] are shown as the green-continuous and the violet-dashed lines, respectively. The experimental data [22] of the ^{9}Be(n,nn)^{8}Be [23] and ^{9}Be(n,α)^{6}He [24] reactions are reported as the red-dotted and blue-dotted-dashed lines, respectively. The $1n$-(S_n), $2n$-(S_{2n}), and α-(S_α) separation energies are also indicated.

PHYSICAL REVIEW C **90**, 064621 (2014)

First application of the n-^{9}Be optical potential to the study of the ^{10}Be continuum via the (^{18}O, ^{17}O) neutron-transfer reaction

D. Carbone,[1,*] M. Bondì,[1,2] A. Bonaccorso,[3] C. Agodi,[1] F. Cappuzzello,[1,2] M. Cavallaro,[1] R. J. Charity,[4] A. Cunsolo,[1] M. De Napoli,[5] and A. Foti[2,5]

INFN Angela Bonaccorso
Istituto Nazionale di Fisica Nucleare
SEZIONE DI PISA

n+^{9}Be

…. SF VMC density & σ_{np} &σ_{pp}-
parametrized according to C. A. Bertulani, and C. De Conti, Phys. Rev. C81 (2010) 064603.
AB phenomenological, DOM

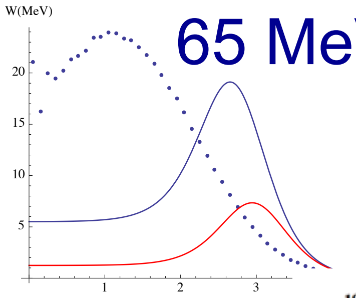

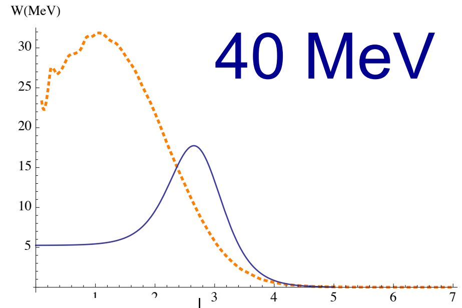

^{9}C+^{9}Be

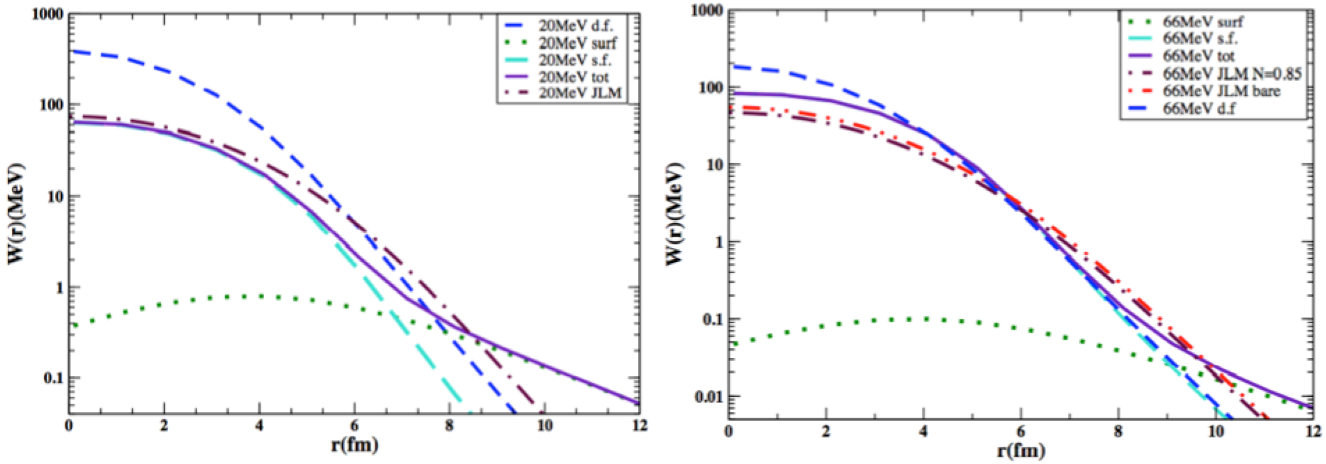

E_{lab}	$J_{d.f.HF}$	rms	J^{ren}_{JLM}	rms	$J^{+surf}_{s.fold}$	rms	$J_{s.fold}$	rms	W_{surf}
(A.MeV)	(MeV fm^3)	(fm)	(MeV fm^3)	(fm)	(MeV fm^3)	(fm)	(MeV)		
20	656	3.55	259	4.42	198	4.72	172	3.81	0.8
38	437	3.55	212	4.40	272	4.29	255	3.85	0.5
66	301	3.55	143	4.31	248	3.96	245	3.86	0.1
83	261	3.55	147	4.27	232.2	3.87	231.7	3.85	0.015

$$W(r) = -4a^i W_{surf} \frac{d}{dr} \frac{1}{1 + e^{(r-R^i)/a^i}}. \qquad (9)$$

with very small strength (W_{surf} =0.8 to 0.015 MeV), the radius has been taken as R^i=3.8 fm, while the diffuseness has been taken large, according to [1; 4], and equal to $a^i = 1/(2\sqrt{2mS_p}/\hbar) = 2$ fm for ^{9}C, since S_p=1.3 MeV.

A. B, and F. Carstoiu, Nucl. Phys. A **706**, 322 (2002).

Angela Bonaccorso

8Li and 8B data from

8. G. W. Fan et al., Phys. Rev. C90 (2014) 044321.
9. M. Fukuda et al., Nucl. Phys. A656 (1999) 209.

9C data from Fukuda, Nishimura, private communication

Cf. **Compound Nucleus Decay with light beams provided by SPES**

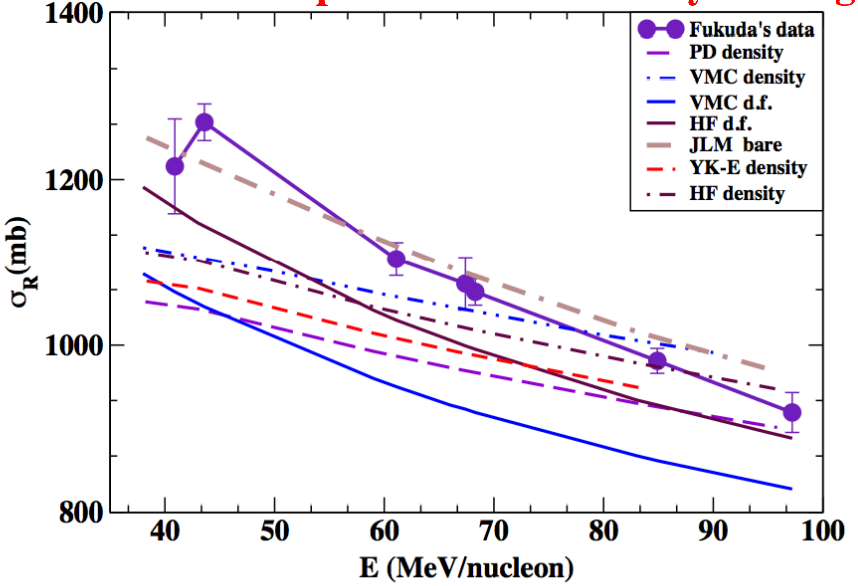

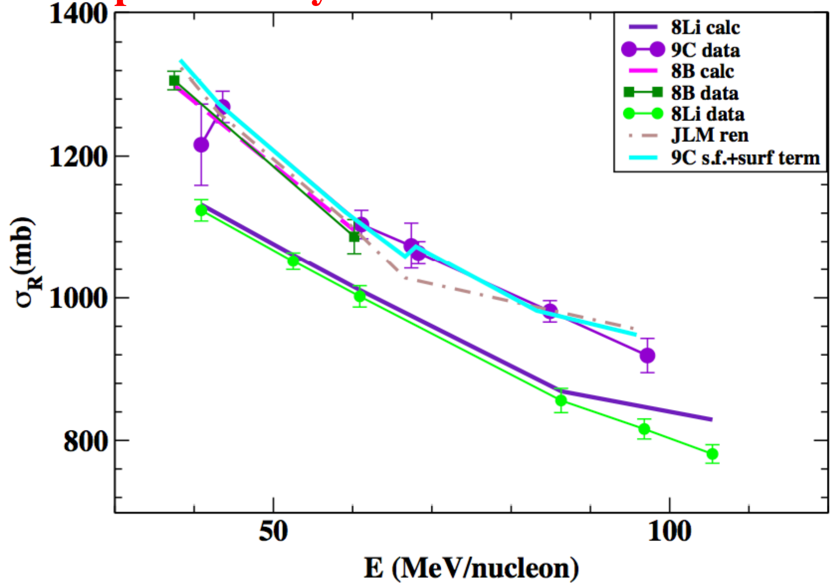

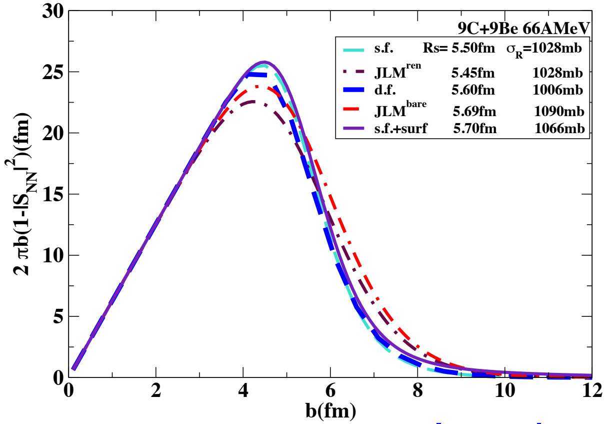

In σ_R large distances are important while breakup is localized around → R_S

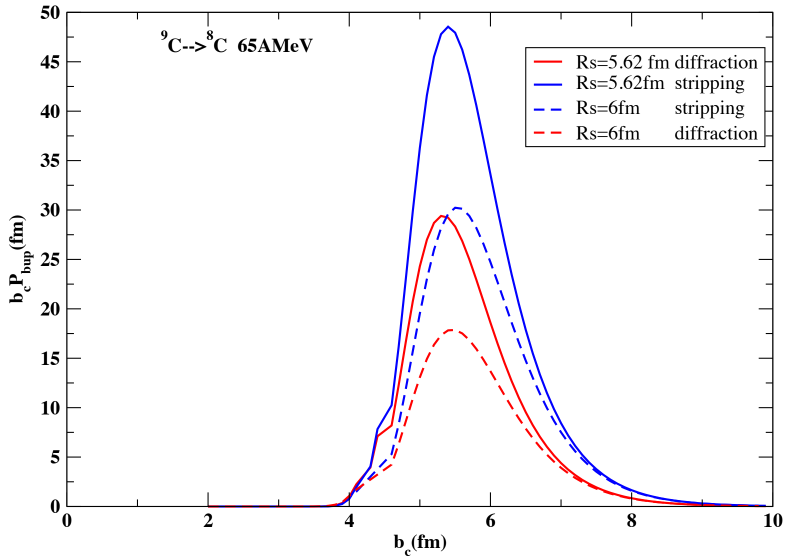

Knockout beyond the dripline

A. Bonaccorso, R. J. Charity, R. Kumar, and G. Salvioni
AIP Conference Proceedings 1645, 30 (2015); doi: 10.1063/1.4909557

TABLE 2. Reaction parameters for the indicated overlaps and cross sections for the corresponding knockout reactions.

	E_{inc} AMeV	σ_{exp} mb	σ_{-n} mb	σ_{-p} mb	$\sigma_{-n_{nop}}$ mb	R_s fm
$\langle {}^7Be \vert {}^6Be_{g.s} \rangle$	65.2	10	(44.7) 68.24		(10.8) 11.12	(6.0) 5.06
$\langle {}^7Be \vert {}^6Li_{g.s} \rangle$	65.2	50		54.4		5.2
$\langle {}^9C \vert {}^8C_{g.s} \rangle$	63.8	3.82	56		(3.86) 42.3 **15**	(6.7) 5.46 **6**
$\langle {}^9C \vert {}^8B_{g.s} \rangle$	64.4	54.5		46		5.3
$\langle {}^9C \vert {}^8B_{1+} \rangle$	64.4	12.2		8.73		5.3
$\langle {}^9C \vert {}^8B_{3+} \rangle$	64.4	42.6		42.3		(5.45)

r_s=1.44 → R_s= 6.00fm → σ_R=15 mb

1.35 5.62 22.8

1.31 5.46 42.3

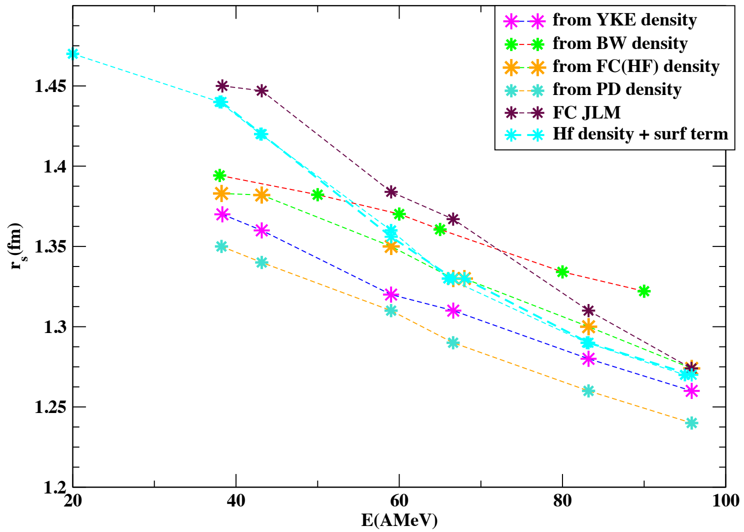

Angela Bonaccorso

N-Z Asymmetry dependence of spectroscopic factors

PHYSICAL REVIEW C 76, 044314 (2007)

Dispersive-optical-model analysis of the asymmetry dependence of correlations in Ca isotopes

R. J. Charity,[1] J. M. Mueller,[2] L. G. Sobotka,[1,2] and W. H. Dickhoff[2]

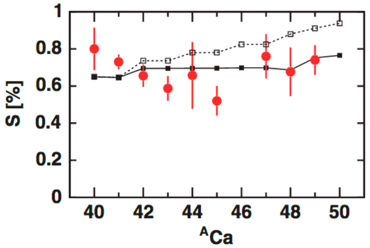

FIG. 14. (Color online) Data points indicate spectroscopic factors deduced by Lee *et al.* [75] for valance neutron hole and particle states in Ca isotopes using (p, d) and (d, p) reactions. The spectroscopic factors are expressed as a percent of the independent-particle-model value. The DOM predictions with the asymmetry dependences D_1 [see Eq. (32)] and D_2 [Eq. (39)] are indicated by the points connected with dashed and solid lines, respectively.

Neutron-Proton Asymmetry Dependence of Spectroscopic Factors in Ar Isotopes

Jenny Lee (李晓菁),[1] M. B. Tsang (曾敏兒),[1] D. Bazin,[1] D. Coupland,[1] V. Henzl,[1] D. Henzlova,[1] M. Kilburn,[1] W. G. Lynch (連致標),[1] A. M. Rogers,[1] A. Sanetullaev,[1] A. Signoracci,[1] Z. Y. Sun (孙志宇),[1,2] M. Youngs,[1] K. Y. Chae,[3] R. J. Charity,[4] H. K. Cheung (張凱傑),[5] M. Famiano,[6] S. Hudan,[7] P. O'Malley,[8] W. A. Peters,[8] K. Schmitt,[3] D. Shapira,[9] and L. G. Sobotka[4]

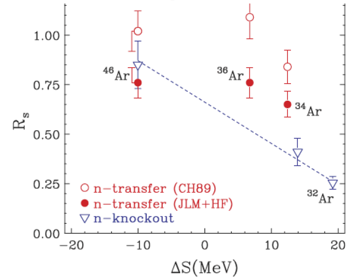

FIG. 2 (color online). Reduction factors $Rs =$ SF(expt)/SF(LB-SM) as a function of the difference between neutron and proton separation energies, ΔS. The solid and open circles represent Rs deduced in JLM + HF and CH89 approach using the present transfer reaction data, respectively. The open triangles denote the Rs from knockout reactions [11]. The dashed line is the best fit of Rs of ^{32,34,46}Ar from knockout reactions. The use of different ΔS values from the present work and knockout reactions in Ref. [11] is explained in Ref. [28].

Quenching of Cross Sections in Nucleon Transfer Reactions

B. P. Kay,[1,2,*] J. P. Schiffer,[1] and S. J. Freeman[3]

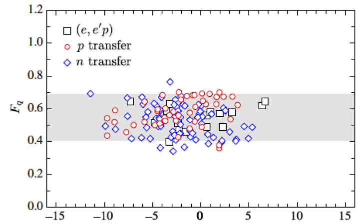

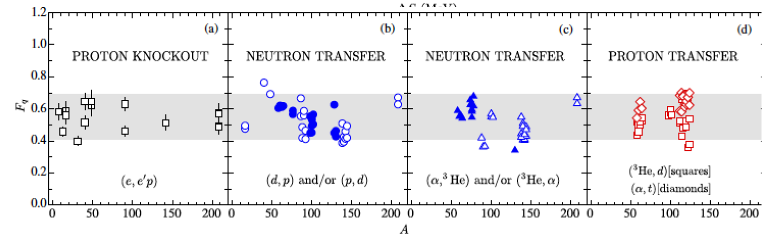

FIG. 1 (color online). The quenching factor F_q versus target mass A. The $(e,e'p)$ data in panel (a) are from Refs. [7,35]. The band represents the mean $\pm 2\sigma$ of the $(e,e'p)$ data to guide the eye. The data in panels (b), (c), (d) are from this analysis and tabulated in the Supplemental Material [26]. Solid symbols are from adding and removing reactions while the empty ones are from

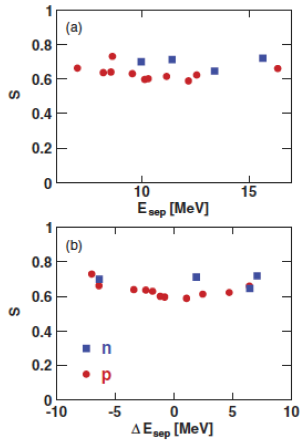

FIG. 27. (Color online) Spectroscopic factors (relative to the independent-particle-model value) for valence-hole levels determined from the fitted potentials. Results are shown for the $Z = 20$, 28 and $N = 28$ and the square and circular points represent neutrons and protons, respectively. In (a), these are plotted versus the separation energy of the level, while in (b), they are plotted versus the difference in proton and neutron separation energies.

PHYSICAL REVIEW C 83, 064605 (2011)

Asymmetry dependence of nucleon correlations in spherical nuclei extracted from a dispersive-optical-model analysis

J. M. Mueller,[1,*] R. J. Charity,[2] R. Shane,[1] L. G. Sobotka,[1,2] S. J. Waldecker,[1] W. H. Dickhoff,[1] A. S. Crowell,[3] J. H. Esterline,[3] B. Fallin,[3] C. R. Howell,[3] C. Westerfeldt,[3] M. Youngs,[4] B. J. Crowe III,[5] and R. S. Pedroni[6]

122503 (2013) PHYSICAL REVIEW LETTERS week ending 22 MARCH 2013

Limited Asymmetry Dependence of Correlations from Single Nucleon Transfer

...y,[1,2] A. Gillibert,[1] L. Nalpas,[1] A. Obertelli,[1] N. Keeley,[3] C. Barbieri,[4] D. Beaumel,[5] S. Boissinot,[1] G. Burgunder,[6] ...lone,[4,7,8] A. Corsi,[1] J. Gibelin,[9] S. Giron,[5] J. Guillot,[5] F. Hammache,[5] V. Lapoux,[1] A. Matta,[5] E. C. Pollacco,[1] R. Raabe,[6,2] M. Rejmund,[6] N. de Séreville,[5] A. Shrivastava,[6] A. Signoracci,[1] and Y. Utsuno[10]

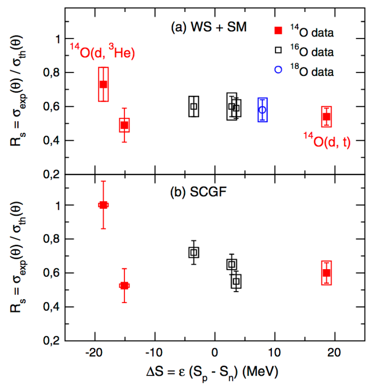

FIG. 4 (color online). Reduction factors R_s obtained with (a) a WS OF and the SLy4 interaction [31], averaged over four entrance and two exit potentials, and compared to shell-model calculations performed with the WBT interaction [37] in the $0p + 2\hbar\omega$ valence space; (b) a microscopic (SCGF) form factor [30]. The detail of error bars is given in text.

Reduction Factors from (p,2p) Cross Sections for $^{14-23}$O Projectiles

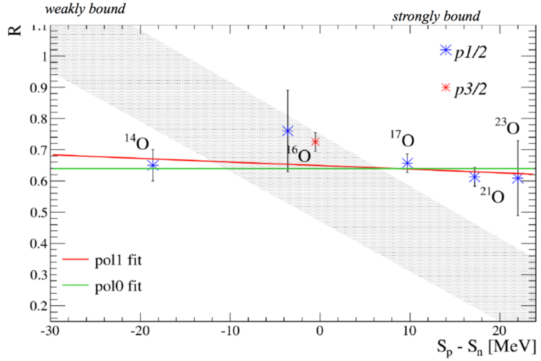

Reduction factor
$R = \sigma_{exp}/\sigma_{theo(IPM)}$

- A weak or no dependence of single-particle strength on the isospin asymmetry
- In contrast to the observed trend from knockout reactions at intermediate energies using composite targets
- Comparable with the ab-initio Green's function and coupled cluster calculations as well as (e,e'p) data

L. Atar, Panin, Paschalis, Aumann, Bertulani et al. for the R3B collaboration

Angela Bonaccorso

Unbound Nuclei "levels"

Available online at www.sciencedirect.com
ScienceDirect
ELSEVIER
Nuclear Physics A 791 (2007) 303–312
NUCLEAR PHYSICS A

^{10}Li spectrum from ^{11}Li fragmentation

G. Blanchon[a], A. Bonaccorso[a,*], D.M. Brink[b], N. Vinh Mau[c]

Table 3
Scattering length of the 2s continuum state, energies and widths of the p- and d-resonances in ^{10}Li and corresponding strength parameters for the δV potential

	ε_{res} (MeV)	Γ_j (MeV)	a_s (fm^{-1})	α (MeV)
$2s_{1/2}$			−17.2	−10.0
$1p_{1/2}$	0.63	0.35		3.3
$1d_{5/2}$	1.55	0.18		−9.8

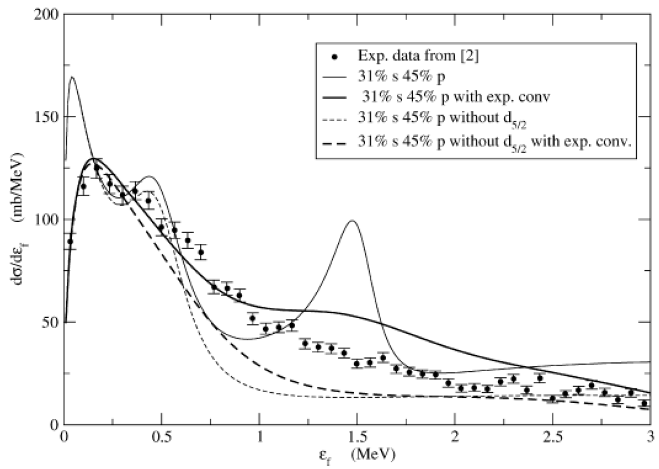

Fig. 2. n–^{9}Li relative energy spectrum, for the reaction $^{11}\mathrm{Li} + {}^{12}\mathrm{C} \to n + {}^9\mathrm{Li} + X$ at 264 A MeV. Only the contributions from an s and p initial state with experimental spectroscopic factors [4] $C^2S = 0.31$ and 0.45 respectively are included. The thin solid curve is the total calculated result. The thick solid curve is after convolution with the experimental resolution function. The thin dashed curve is the calculation without the d-resonance while the thick dashed curve is the same calculation after convolution. The symbols with error bars are the experimental points from [2]. Calculations are normalised to the data.

H. Simon et al., NPA791, 267 (2007)

Physics Letters B 755 (2016) 481–485
Contents lists available at ScienceDirect
Physics Letters B
www.elsevier.com/locate/physletb
ELSEVIER

Investigation of the role of ^{10}Li resonances in the halo structure of ^{11}Li through the ^{11}Li(p, d)^{10}Li transfer reaction

CrossMark

A. Sanetullaev[a,b,1], R. Kanungo[a,*], J. Tanaka[c], M. Alcorta[b], C. Andreoiu[d], P. Bender[b], A.A. Chen[e], G. Christian[b], B. Davids[b], J. Fallis[b], J.P. Fortin[a,f], N. Galinski[b], A.T. Gallant[b], P.E. Garrett[g], G. Hackman[b], B. Hadinia[g], S. Ishimoto[h], M. Keefe[a], R. Krücken[b,i], J. Lighthall[b], E. McNeice[e], D. Miller[b], J. Purcell[a], J.S. Randhawa[a], T. Roger[j], A. Rojas[b], H. Savajols[j], A. Shotter[k], I. Tanihata[c,l], I.J. Thompson[m], C. Unsworth[b], P. Voss[d], Z. Wang[b,d]

The resonance energy spectrum (Fig. 2b) of ^{10}Li is constructed in the missing mass technique using the measured energy and scattering angle of the deuterons. A very prominent resonance peak is seen at $E_r = 0.62 \pm 0.04$ MeV and full width $\Gamma = 0.33 \pm 0.07$ MeV is obtained from fitting the spectrum with a Voigt function with an energy dependent Breit–Wigner function width [22].

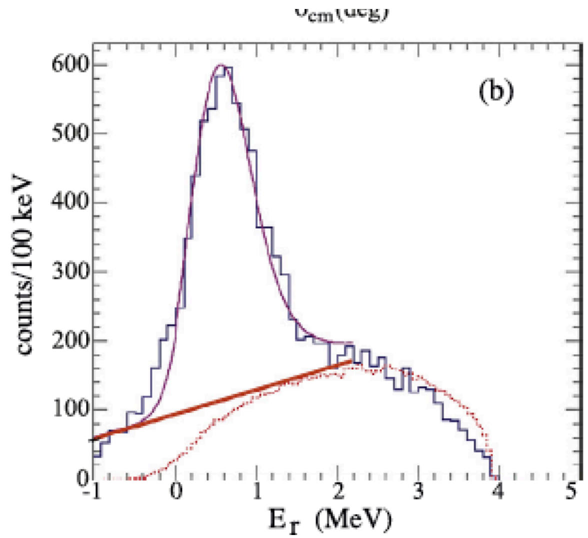

Flagships are still flagship!!!!

(Uesaka san)

INFN Angela Bonaccorso
Istituto Nazionale di Fisica Nucleare
SEZIONE DI PISA

State-of-the-art (recent progress)

Traditional methods

- Renewed interest in higly numerical DWBA and CDCC calculations of various aspects of breakup: A. Moro & Co., B.V. Carlson et al., K.Ogata et al. So far mainly d-induced reactions.
- Resonant scattering and R-matrix: P. Descouvemont, G. Rogachev, A. Di Pietro et al.
- Various eikonal approaches: best recent results (p,pN): Bertulani-Aumann for R3B collaboration.
- Semiclassical and few body (Hussein, Canto &Co), P. Capel
- Reaction cross sections OK with eikonal approach (Ogawa): improved folding models for the optical potential (Furumoto opt pot)

New methods:

- Chiral interactions used for: ab initio no-core shell model with continuum, and its applications to nucleon and deuterium scattering on light nuclei: P. Navratil, S. Quaglioni, G. Hupin, J. Dohet-Eraly
- Optical potential microscopic calculations from chiral interactions

ECT* workshop

Towards consistent approaches for nuclear structure and reactions
06 Jun 2016 to 10 Jun 2016
Poster Program
Organizers
Carlos Bertulani (Texas A&M University-Commerce) carlos.bertulani@tamuc.edu
Guillaume Blanchon (CEA - DAM - DIF) guillaume.blanchon@cea.fr
Gregory Potel (Lawrence Livermore National Laboratory) potel@nscl.msu.edu
Vittorio Soma (CEA Saclay) vittorio.soma@cea.fr

Open questions:

- Unbound nuclei via projectile fragmentation. SEMICLASSICAL OK, but numerical (DWBA-like still in progress)
- Tetraneutron

Physics beyond the limits of stability: exploring the continuum
17 Oct 2016 to 21 Oct 2016
Organizers
Angela Bonaccorso (INFN Pisa) angela.bonaccorso@pi.infn.it
Nigel Orr (LPC Caen) orr@lpccaen.in2p3.fr

INFN Angela Bonaccorso
Istituto Nazionale di Fisica Nucleare

Nuclei are not anymore what they used to be . . .
Re-write Nuclear Physics Textbooks !!

- $R=1.4\text{-}1.5\,(A_p^{1/3}+A_t^{1/3})$fm…….radius

- NN Optical potentials (imag. part) describing elastic scattering and/or reaction cross sections must contain a surface term with very large diffusness 2-3fm.

- nN optical potentials (real part) must contain a term representing particle-vibration couplings or surface oscillations/deformations, consistent with a dispersive contribution **DOM** $\delta V(r) = 16\alpha \frac{e^{2(r-R^R)/a^R}}{(1+e^{(r-R^R)/a^R})^4}.$ "shape"

- Bound&continuum

- Energy dependence ? http://pdg.lbl.gov/2015/reviews/rpp2015-rev-cross-section-plots.pdf

50. Plots of cross sections and related quantities 11

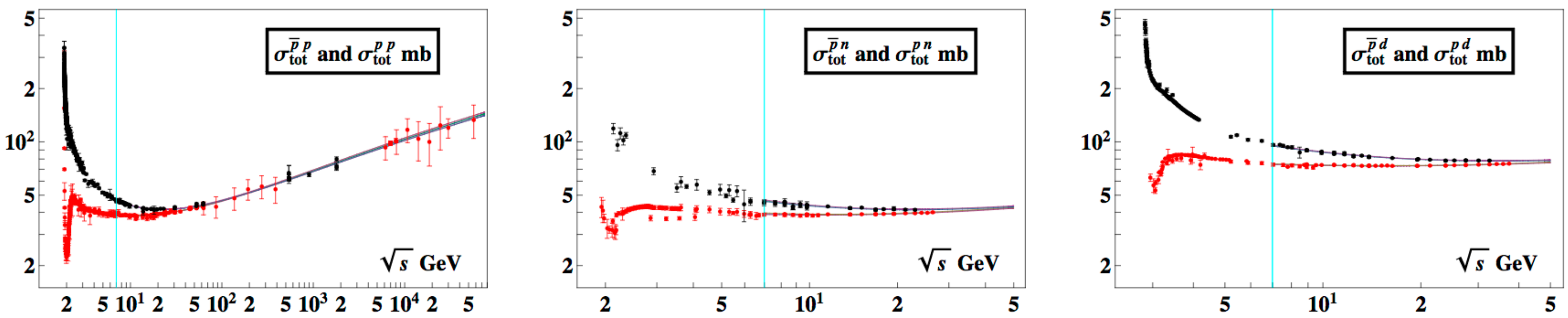

INFN Angela Bonaccorso
Istituto Nazionale di Fisica Nucleare
SEZIONE DI PISA

Outlook

What next for 2017-2050?

- Understanding at a microscopic level the **energy dependence** of nn and NN interactions, including optical potentials.
- **Surface effects, clustering** and **unbound structures** →
  Will eventually nuclear physics become the study of unbound nuclei via resonance definition, similarly to particle physics, nuclear matter, neutron stars, plasma?
- Structure and reaction models will be unified via ab-initio methods and full inclusion of continuum spectra.
  - Will improvements in numerical techniques allow to solve the nuclear many body problem "exactly"?

and/or

will semiclassical and/or analytical methods survive.

"If you have heart you will certainly have brain…"
(paraphrased from Julian Fellowes)

Courtesy of R J Charity : Egret at dawn in Beachmere Australia

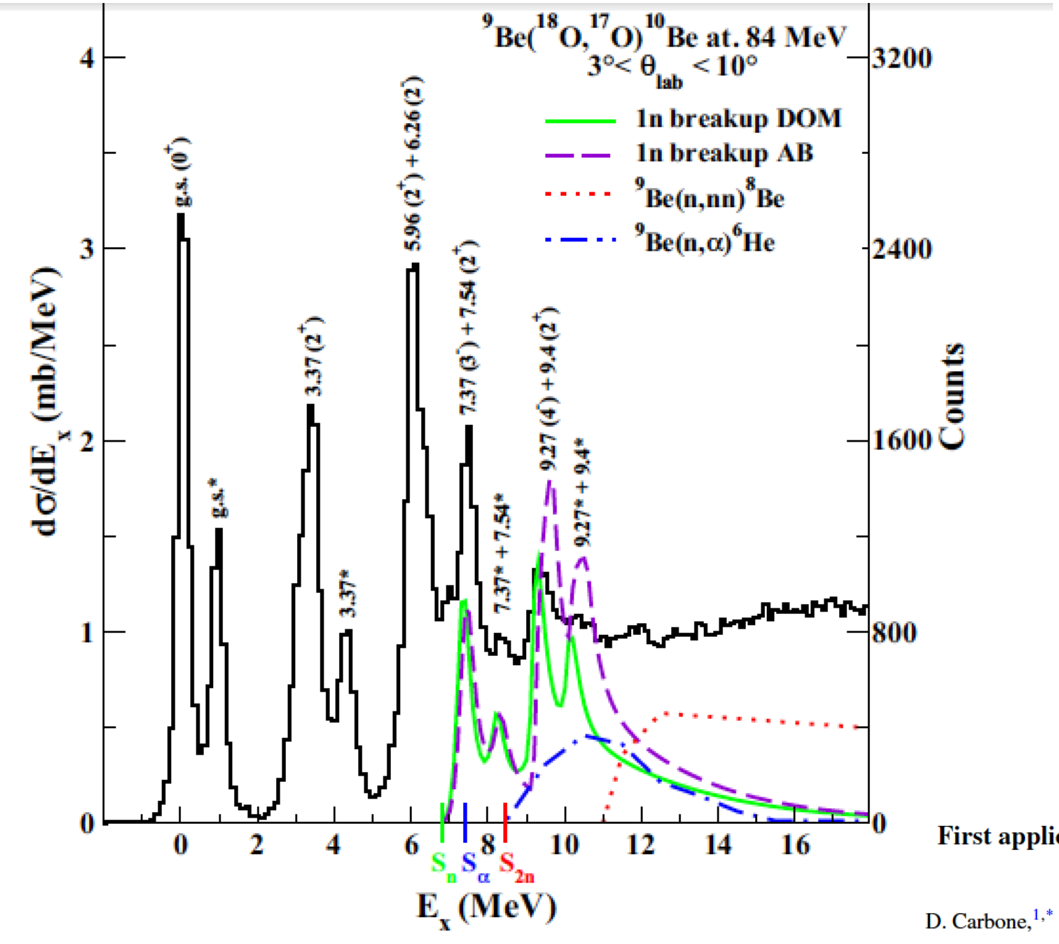

FIG. 2. (Color online) Inclusive excitation energy spectrum of the ^{9}Be(^{18}O,^{17}O)^{10}Be reaction at 84-MeV incident energy and $3^\circ < \theta_{\mathrm{lab}} < 10^\circ$. The background that comes from ^{12}C and ^{16}O impurities has been subtracted. Peaks marked with an asterisk refer to the ^{17}O ejectile emitted in its first excited state at 0.87 MeV. Total $1-n$ breakup calculations that result from the use of the DOM and the AB potentials (see text) [12] are shown as the green-continuous and the violet-dashed lines, respectively. The experimental data [22] of the ^{9}Be(n,nn)^{8}Be [23] and ^{9}Be(n,α)^{6}He [24] reactions are reported as the red-dotted and blue-dotted-dashed lines, respectively. The $1n$-(S_n), $2n$-(S_{2n}), and α-(S_α) separation energies are also indicated.

PHYSICAL REVIEW C **90**, 064621 (2014)

First application of the n-^{9}Be optical potential to the study of the ^{10}Be continuum via the (^{18}O,^{17}O) neutron-transfer reaction

D. Carbone,[1,*] M. Bondì,[1,2] A. Bonaccorso,[3] C. Agodi,[1] F. Cappuzzello,[1,2] M. Cavallaro,[1] R. J. Charity,[4] A. Cunsolo,[1] M. De Napoli,[5] and A. Foti[2,5]

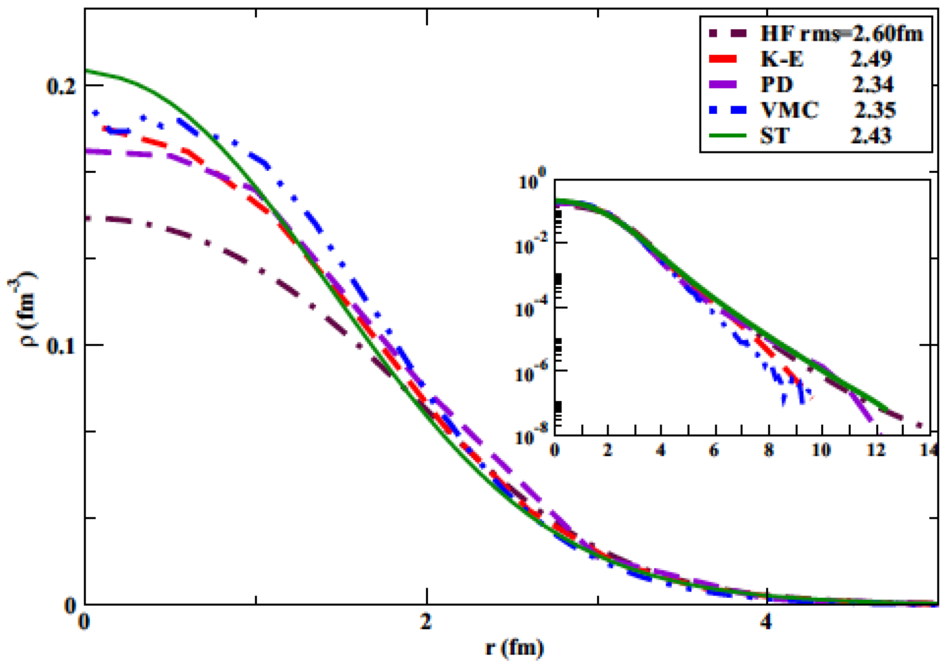

FIG. 4. ^{9}C densities used in the calculated cross sections shown in Fig. 2.

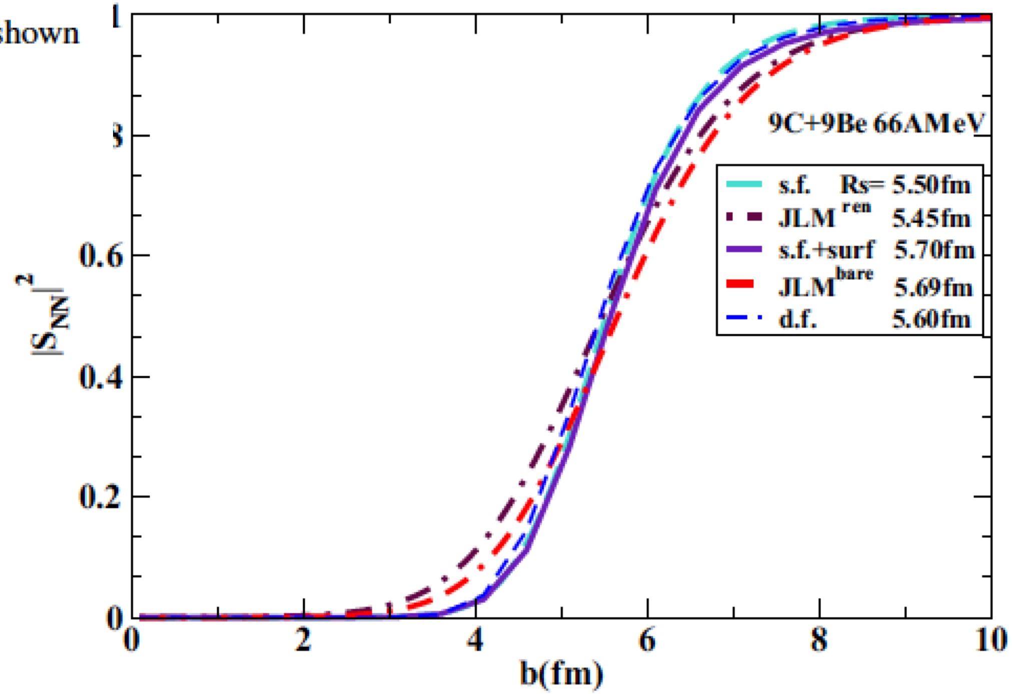

TABLE II. Experimental reaction cross sections, second column, from Ref. [32]. Calculated total reaction cross sections with the double-folded potential using VMC densities for both ^{9}C and ^{9}Be (third column); double-folded potential using HF densities for both ^{9}C and ^{9}Be (fourth column); using the single-folded potential with HF density for ^{9}C (fifth column) and with the added surface potential (sixth column), with the "bare" JLM and with the renormalized JLM for $^9\mathrm{C} + {}^9\mathrm{Be}$. The renormalization factor for the JLM potential and strength of the additional surface potential for the single-folded potential are also given. For the case of $\sigma^{+\mathrm{surf}}_{\mathrm{s.fold}}$ we then give strong-absorption radius R_s from $|S_{NN}(R_s)|^2 = \frac{1}{2}$, and R_S^{fit} from the fit to the calculated $|S_{NN}|^2$ according to Eq. (10). In this case also the diffuseness-like parameter is given. Last column: r_s from Eq. (11) and R_s.

E_{lab} (MeV/nucleon)	σ_{exp} (mb)	$\sigma^{\mathrm{VMC}}_{\mathrm{d.fold}}$ (mb)	$\sigma^{\mathrm{HF}}_{\mathrm{d.fold}}$ (mb)	$\sigma_{\mathrm{s.fold}}$ (mb)	$\sigma^{+\mathrm{surf}}_{\mathrm{s.fold}}$ (mb)	$\sigma^{\mathrm{bare}}_{\mathrm{JLM}}$ (mb)	$\sigma^{\mathrm{ren}}_{\mathrm{JLM}}$ (mb)	N_{JLM}	W_{surf} (MeV)	R_s (fm)	R_s^{fit} (fm)	a^{fit} (fm)	r_s (fm)
20		1267	1409	1078	1565	1338	1538	1.65	0.8	6.12	6.25	1.01	1.47
38		1086	1191	1112	1341	1250	1324	1.20	0.5	5.95	5.99	0.97	1.44
40.9	1216 ± 57	1064	1166	1117	1291	1235	1215	0.95	0.4	5.95	5.99	0.98	1.44
43		1050	1148	1103	1275	1221	1260	1.10	0.4	5.95	5.99	0.99	1.44
43.6	1269 ± 22	1046	1144	1106	1235	1219	1257	1.10	0.3	5.82	5.70	0.80	1.40
59		960	1042	1047	1124	1130	1111	0.95	0.2	5.70	5.64	0.82	1.36
61.1	1104 ± 20	950	1030	1045	1122	1119	1119	1.00	0.2	5.68	5.63	0.83	1.36
66		928	1006	1028	1066	1091	1028	0.85	0.1	5.60	5.55	0.80	1.35
67.4	1074 ± 32	923	999	1026	1056	1087	1087	1.00	0.08	5.60	5.53	0.80	1.35
68.3	1064 ± 16	919	995	1024	1052	1082	1063	0.95	0.075	5.55	5.49	0.80	1.33
83		867	934	948	979	1015	987	0.93	0.015	5.40	5.38	0.78	1.29
84.9	981 ± 15	861	928	979	983	1008	989	0.95	0.01	5.40	5.36	0.80	1.29
95		833	895	949	952	968	956	0.97	0.01	5.40	5.28	0.79	1.29
97.2	919 ± 24	827	888	949	951	963	923	0.90	0.005	5.35	5.28	0.80	1.28

INFN Angela Bonaccorso
Istituto Nazionale di Fisica Nucleare
Sezione di Pisa

I.Tanihata, "HOW IT ALL STARTED"

Focus Point
in EPJ+, 131 4 (2016) 90
Re-writing Nuclear Physics textbooks: 30 years of radioactive ion beam physics
DOI: 10.1140/epjp/i2016-16090-x

http://exotic2015.df.unipi.it/

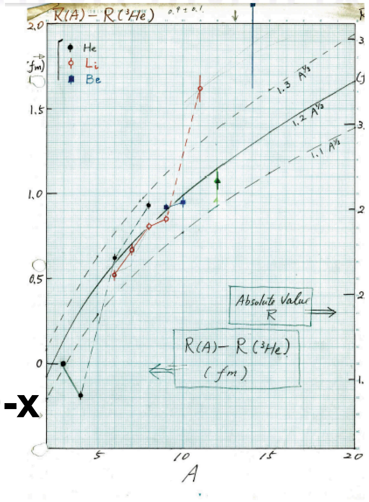

Fig. 11 The firstly determined radii of He, Li, and
isotope radii. *R* in this figure is R_I in the text.

Early experiments: halo nuclei

I. Tanihata et al., Phys. Lett. B 160, 380 (1985)

$$\sigma_R = \pi\left(R_{vol} + R_{surf}\right)^2\left(1 - \frac{B_c}{E_{cm}}\right)$$

Kox et al. (1987)

$$\sigma_I = \pi\,[R_I(P) + R_I(T)]^2$$

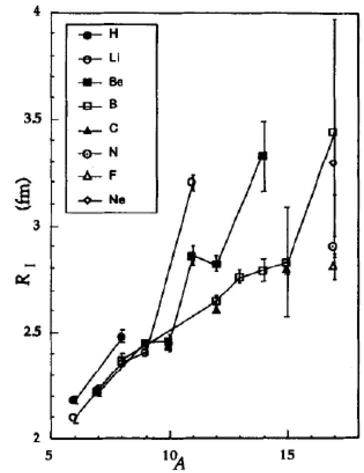

Early theory: halo nuclei
P. G. Hansen and B. Jonson,
Europhys. Lett., 4, 409 (1987)

Early eikonal model

I. Tanihata, Prog. Part. Nucl. Phys. 35, 505 (1995)

These equations provide a simple way to compare the reaction cross sections at different energies. However, since they are purely empirical formula, one should be careful when applying them to an exotic nucleus because of a possible difference in the surface diffuseness as well as any proton-neutron density difference. When one measures σ_R using a β-unstable nucleus, only r_0 is expected to change.

$$\sigma_R = \int_0^\infty d\mathbf{b}\left(1 - |S(\mathbf{b})|^2\right) = \sigma_{ct} + \sigma_{nt}$$

decoupling of core and halo

$$|S(\mathbf{b})|^2 = |S_{ct}|^2 |S_{nt}|^2 = |S_{ct}|^2 - |S_{ct}|^2 |S_{nt}|^2$$

$$|S(\mathbf{b})|^2 = e^{-[\sigma_{nn}\int ds\,\rho_p(|b-s|)\rho_t(s)]} = e^{-[\sigma_{nn}\int ds\,\rho_c\rho_t]}\,e^{-[\sigma_{nn}\int ds\,\rho_n\rho_t]}$$

$$\sigma_{nt} = \int_0^\infty d\mathbf{b}\,|S_{ct}|^2 P_{bup}$$

INFN Angela Bonaccorso
Istituto Nazionale di Fisica Nucleare
SEZIONE DI PISA

Light-medium mass nuclei. Direct reactions, exotic decays, delayed particles.